THE JOURNAL OF BIOLOGICAL CHEMISTRY VOL. 287, NO. 30, pp. 25615–25630, July 20, 2012

Polydom/SVEP1 Is a Ligand for Integrin $\alpha9\beta1$*[S]

Received for publication, February 21, 2012, and in revised form, May 14, 2012 Published, JBC Papers in Press, May 31, 2012, DOI 10.1074/jbc.M112.355016

Ryoko Sato-Nishiuchi[‡], Itsuko Nakano[‡], Akio Ozawa[‡], Yuya Sato[‡], Makiko Takeichi[‡], Daiji Kiyozumi[‡], Kiyoshi Yamazaki[§], Teruo Yasunaga[§], Sugiko Futaki[‡], and Kiyotoshi Sekiguchi[‡1]

From the [‡]Institute for Protein Research and [§]Research Institute for Microbial Disease, Osaka University, Suita, Osaka 565-0871, Japan

Background: Polydom/SVEP1 is a putative extracellular matrix protein of unknown function.
Results: Polydom/SVEP1 is a potent ligand for integrin $\alpha9\beta1$ and colocalizes with the integrin *in vivo*.
Conclusion: Polydom/SVEP1 is a hitherto unknown high affinity ligand for integrin $\alpha9\beta1$.
Significance: The identification of this high affinity ligand offers important clues toward better understanding of the consequences of integrin $\alpha9\beta1$-mediated cell-extracellular matrix interactions.

A variety of proteins, including tenascin-C and osteopontin, have been identified as ligands for integrin $\alpha9\beta1$. However, their affinities for integrin $\alpha9\beta1$ are apparently much lower than those of other integrins (*e.g.* $\alpha3\beta1$, $\alpha5\beta1$, and $\alpha8\beta1$) for their specific ligands, leaving the possibility that physiological ligands for integrin $\alpha9\beta1$ still remain unidentified. In this study, we found that polydom (also named SVEP1) mediates cell adhesion in an integrin $\alpha9\beta1$-dependent manner and binds directly to recombinant integrin $\alpha9\beta1$ with an affinity that far exceeds those of the known ligands. Using a series of recombinant polydom proteins with N-terminal deletions, we mapped the integrin-binding site to the 21st complement control protein domain. Alanine-scanning mutagenesis revealed that the EDDMMEVPY sequence (amino acids 2636–2644) in the 21st complement control protein domain was involved in the binding to integrin $\alpha9\beta1$ and that Glu^{2641} was the critical acidic residue for the integrin binding. The importance of this sequence was further confirmed by integrin binding inhibition assays using synthetic peptides. Immunohistochemical analyses of mouse embryonic tissues showed that polydom colocalized with integrin $\alpha9$ in the stomach, intestine, and other organs. Furthermore, *in situ* integrin $\alpha9\beta1$ binding assays using frozen mouse tissues showed that polydom accounts for most, but not all, of the integrin $\alpha9\beta1$ ligands in tissues. Taken together, the present findings indicate that polydom is a hitherto unknown ligand for integrin $\alpha9\beta1$ that functions as a physiological ligand *in vivo*.

Integrins comprise a diverse family of cell surface receptors that mediate the adhesive interactions of cells with extracellular matrices (ECMs)[2] as well as other cells. Each integrin is composed of a pair of α and β subunits, which both span the plasma membrane and are noncovalently associated with one another. In mammals, 18 α subunits and eight β subunits have been identified to form 24 integrin heterodimers, each with distinct ligand specificities depending on the subunit combinations (1). For example, integrins $\alpha1\beta1$ and $\alpha2\beta1$ bind to collagens; $\alpha3\beta1$, $\alpha6\beta1$, $\alpha7\beta1$, and $\alpha6\beta4$ bind to laminins; and $\alpha5\beta1$-, $\alpha8\beta1$-, $\alpha IIb\beta3$-, and αV-containing integrins bind to a variety of Arg-Gly-Asp (RGD)-containing ligands, such as fibronectin, nephronectin, and vitronectin.

Integrin $\alpha9\beta1$ is widely expressed in both adult and embryonic tissues, including airway epithelium, the basal layer of squamous epithelium, smooth muscle, skeletal muscle, hepatocytes, and corneal epithelia (2–4). Mice deficient in integrin $\alpha9$ expression develop chylothorax and respiratory failure and die between 6 and 12 days after birth (5). Integrin $\alpha9\beta1$ is also expressed in the endothelial cells of lymphatic valves, and endothelial cell-specific depletion of integrin $\alpha9$ in mouse embryos results in failure of lymphatic valve development, suggesting a role for integrin $\alpha9\beta1$ in lymphatic valve morphogenesis (6). Recent studies on skin-specific knockout of integrin $\alpha9\beta1$ revealed a crucial role for the integrin in re-epithelialization during cutaneous wound healing (7).

A panel of ECM proteins, including tenascin-C, osteopontin, and the fibronectin isoform containing an EIIIA domain have been shown to bind to integrin $\alpha9\beta1$ (8–10). Some membrane proteins (ADAM proteases and vascular cell adhesion molecule (VCAM)-1) and growth factors (VEGF and NGF) have also been reported as ligands for integrin $\alpha9\beta1$ (11–14). However, it remains to be explored whether these proteins function as integrin $\alpha9\beta1$ ligands in a physiological context. For example, integrin $\alpha9\beta1$ bound to the N-terminal fragment or polymeric form of osteopontin, but not to the intact protein, and also bound to the EIIIA domain of fibronectin, but not to a longer fragment (15–17). Furthermore, the binding specificities of these ligands have often been based on cell adhesion assays using integrin $\alpha9$-expressing cells and/or cell adhesion inhibition assays with anti-integrin $\alpha9$ antibodies (8–14). Direct

* This study was supported in part by Grant-in-Aid for Scientific Research on Innovative Areas 22122006 and Research Contracts 06001294-0 and 10001843-0 with the New Energy and Industrial Technology Development Organization of Japan.

[S] This article contains supplemental Figs. S1–S6.

[1] To whom correspondence should be addressed: Laboratory of Extracellular Matrix Biochemistry, Institute for Protein Research, Osaka University, 3-2 Yamadaoka, Suita, Osaka 565-0871, Japan. Tel.: 81-6-6879-8617; Fax: 81-6-6879-8619; E-mail: sekiguch@protein.osaka-u.ac.jp.

[2] The abbreviations used are: ECM, extracellular matrix; CCP, complement control protein; TNfn3, third fibronectin type III repeat of tenascin-C; OPN-Nhalf, N-terminal fragment of osteopontin; VCAM, vascular cell adhesion molecule; Ni-NTA, nickel-nitrilotriacetic acid; MIDAS, metal ion-dependent adhesion site; E*n*, embryonic day *n*; ADAM, a disintegrin and metalloproteinase.

integrin α9β1 binding assays have also been employed for tenascin-C, osteopontin, VCAM-1, VEGF, and NGF (13, 14, 16, 18), although no comparative analyses of the affinities of these ligands toward integrin α9β1 have been performed.

In this study, we identified polydom, a putative ECM protein containing an array of complement control protein (CCP) domains along with a von Willebrand factor A domain, a pentraxin domain, and multiple EGF-like domains, as another ligand for integrin α9β1. Polydom was originally identified in murine bone marrow stromal cells as a protein containing EGF-like domains that share strong similarities with those in the Notch family proteins (19). The human orthologue of polydom, named SVEP1/SEL-OB, was reported as a protein expressed on the surface of osteogenic cells (20). We encountered polydom in our *in silico* screening for functionally unknown ECM proteins (21). Using recombinant expression and *in vitro* cell adhesion assays, we found that polydom is a secreted protein that mediates cell adhesion in an integrin α9β1-dependent manner. Our findings show that polydom is a hitherto unknown α9β1 ligand with an affinity that far exceeds those of the known α9β1 ligands. Furthermore, polydom colocalizes with integrin α9β1 in mouse tissues, supporting its role as a physiological ligand for integrin α9β1.

EXPERIMENTAL PROCEDURES

Cells, Antibodies, and Reagents—RD human rhabdomyosarcoma cells, A549 human lung adenocarcinoma cells, and HT1080 human fibrosarcoma cells were maintained in DMEM supplemented with 10% FBS. Freestyle™ 293-F cells were obtained from Invitrogen and cultured in Freestyle 293-F expression medium (Invitrogen). Mouse mAbs against human integrin α3 (3G8) and α5 (8F1) were raised in our laboratory as described previously (22, 23). An mAb against integrin α6 (AMCI7-4) was provided by Dr. Masahiko Katayama (Eisai Co., Ltd., Tsukuba, Japan) (24). An mAb against human integrin β1 (AIIB2) developed by Dr. Caroline Damsky (University of California, San Francisco, CA) was obtained from the Developmental Studies Hybridoma Bank (Iowa City, IA). Mouse mAbs against human integrin α2 (P1E6) and integrin α9β1 (Y9A2) and mouse normal IgG were purchased from Santa Cruz Biotechnology, Inc. (Santa Cruz, CA). A goat polyclonal antibody against mouse integrin α9 was obtained from R&D Systems (Minneapolis, MN). A rat mAb against mouse tenascin-C (MTn-12) was purchased from Sigma. An HRP-conjugated anti-FLAG® M2 antibody and an anti-penta-His antibody were obtained from Sigma and Qiagen (Valencia, CA), respectively. Alexa Fluor™-conjugated antibodies and an APEX™ Alexa Fluor antibody labeling kit were purchased from Invitrogen. An anti-"Velcro" antibody was raised in rabbits by immunization with coiled-coil ACID and BASE peptides as described (25). Human plasma fibronectin and recombinant cellular fibronectin containing the EDA, EDB, and IIICS regions were purified as described previously (26, 27). Synthetic peptides were purchased from Thermo Fisher Scientific (Ulm, Germany). An siRNA mixture targeting human integrin α9 (catalog no. SHF27A-2214) and a negative control siRNA mixture (catalog no. C6A-0126) were purchased from COSMO BIO (Tokyo, Japan). The integrin α9 mixture contained three siRNAs: 5′-GGACAUGGCUCGAGGGAAG-3′, 5′-GUCCAUAUCGGGAGGCAUU-3′, and 5′-CCCUAAGGGUGGUGGAAAU-3′.

cDNA Cloning and Construction of Expression Vectors—DNA segments encoding a FLAG tag and a His_6 tag were PCR-amplified and inserted into the NotI/ApaI sites of the pcDNA3.1(+) or pSecTag 2B vector (Invitrogen), yielding pcDNA-FLAG, pSec-FLAG, and pSec-His. For construction of expression vectors for N-terminal FLAG-tagged proteins, the DNA segment encoding the FLAG sequence was inserted into the HindIII/BamHI sites of the pSec-His vector to yield pSec-NFLAG-His. A cDNA encoding mouse polydom was obtained by RT-PCR using RNA extracted from mouse embryos at embryonic day 17 (E17) (Clontech, Palo Alto, CA) and subcloned into pBluescript® KS(+) (Stratagene, La Jolla, CA). After sequence verification, error-free cDNA fragments were inserted into pcDNA-FLAG, pSec-FLAG, pSec-His, or pSec-NFLAG-His at the BamHI/NotI sites. Expression vectors for truncated forms of polydom were also constructed by subcloning of PCR-amplified cDNAs into pSec-His at BamHI/NotI or HindIII/NotI sites.

Expression and Purification of Recombinant Polydom Proteins—Recombinant polydom and its fragments were produced using the FreeStyle 293 Expression System (Invitrogen). FreeStyle 293-F cells were transfected with the expression vectors using 293fectin (Invitrogen) and grown in serum-free FreeStyle 293 expression medium for 72 h. The conditioned media were collected and clarified by centrifugation. To check the expression, the cells were lysed with TBS containing 1% (w/v) Nonidet P-40, 1 mM PMSF, 5 μg/ml aprotinin, 5 μg/ml leupeptin, and 5 μg/ml pepstatin. The conditioned media and cell lysates were pulled down using Ni-NTA-agarose (Qiagen) or anti-FLAG M2-agarose (Sigma), respectively, and subjected to immunoblotting. For purification of the FLAG-tagged proteins, the conditioned media were applied to an anti-FLAG M2-agarose column, and the bound proteins were eluted with 100 μg/ml FLAG peptide in PBS. For purification of the His-tagged proteins, the conditioned media were subjected to affinity chromatography using Ni-NTA-agarose. The columns were washed with PBS, and the bound proteins were eluted with PBS containing 200 mM imidazole. The eluted proteins were dialyzed against PBS. The concentrations of the purified proteins were determined by the Bradford assay using BSA as a standard.

Anti-polydom Antibodies—Antibodies against polydom were raised in rabbits using FLAG-tagged full-length polydom as an immunogen. The antibodies were affinity-purified on columns containing either the N-terminal or C-terminal polydom fragment, designated pol-N (amino acids 18–789) and pol-C (amino acids 1192–3567), respectively, with a C-terminal His_6 tag. The columns were washed with 10 mM Tris-HCl buffer (pH 7.5) containing 0.5 M NaCl, followed by elution of the bound antibodies with 0.1 M glycine-HCl (pH 2.8). The eluted fractions were immediately neutralized with 1 M Tris-HCl (pH 9.0) and dialyzed against PBS. An Alexa Fluor 555-conjugated anti-polydom (pol-N) antibody was prepared using the APEX Alexa Fluor antibody labeling kit.

SDS-PAGE, Western Blotting, and Amino Acid Sequencing—SDS-PAGE was carried out according to Laemmli (28). The separated proteins were visualized by staining with silver

nitrate or Coomassie Brilliant Blue or transferred onto nitrocellulose (for immunoblotting) or polyvinylidene difluoride (for amino acid sequencing) membranes. For immunoblotting, the membranes were probed with antibodies and then visualized with an ECL detection kit (GE Healthcare). For amino acid sequencing, the protein bands on the membrane were visualized by Coomassie Brilliant Blue staining and then dissected out. The N-terminal amino acid sequences were analyzed by the method of Edman (29) using a Procise 491 cLC protein sequencer (Applied Biosystems, Carlsbad, CA).

Preparation of Tissue Extracts—Mouse E15.5 lungs were homogenized in SDS-PAGE sample buffer (2% SDS, 10% glycerol, 125 mM Tris-HCl, pH 6.8), and the protein concentrations of the homogenates were determined using a BCA protein assay reagent kit (Pierce). The homogenates were boiled, and the extracted proteins were subjected to SDS-PAGE and Western blotting.

Cell Adhesion Assays—Cell adhesion assays were performed as described (30). For the assays involving blocking antibodies, RD cells were preincubated with the specified mAbs (10 μg/ml) for 15 min at room temperature and plated on 96-well plates coated with recombinant polydom proteins or fibronectin. The cells were incubated for 30 min, washed, fixed with 3.7% formaldehyde, and stained with 0.5% toluidine blue.

Flow Cytometry—The integrin α9β1 expression levels on A549, HT1080, and RD cells were verified by flow cytometry using anti-integrin α9β1 mAb Y9A2. Mouse normal IgG was used as a control.

RNA Interference—RD cells were grown on 6-well plates in DMEM containing 10% FBS. The cells were transfected with 30 pmol of siRNA using Lipofectamine™ RNAiMAX (Invitrogen). After 5 h, the cells were passaged into 10-cm dishes. At 3 days after transfection, the cells were subjected to flow cytometry or cell adhesion assays.

Expression and Purification of Recombinant Integrins—A cDNA encoding the extracellular region of human integrin α9 was amplified by RT-PCR using total RNA extracted from RD cells and cloned into pBluescript KS(+). After sequence verification, an error-free cDNA fragment was inserted into pcDNA-ACID-FLAG (31). An expression vector for the extracellular regions of integrin β1 was provided by Dr. Junichi Takagi (Osaka University, Osaka, Japan) (25). The recombinant integrins were produced using the FreeStyle 293 expression system and purified as described (31).

Integrin Binding Assay—Integrin binding assays were performed as described previously (31). In some experiments, integrins were preincubated with synthetic peptides at various concentrations to evaluate their inhibitory activities. The apparent dissociation constants were determined as described (32).

Expression and Purification of GST-fused Polydom, Tenascin-C, and Osteopontin Fragments—cDNAs encoding the 21st CCP domain or its deletion mutants were amplified by PCR and subcloned into pGEX4T-1 (GE Healthcare) at the EcoRI/SalI sites. The 21st CCP domain and the same domain lacking the Glu^{2628}–Ser^{2664} segment, designated ΔD2628-S2664, were His_6-tagged at their C termini. GST fusion proteins were induced in *Escherichia coli* BL21 by incubation with 0.1 mM isopropyl β-D-thiogalactopyranoside at 25 °C for 2 h. The cells were lysed by sonication, and the supernatants were passed over a glutathione-Sepharose 4B (GE Healthcare) column. The bound proteins were eluted with 50 mM Tris-HCl (pH 8.0) containing 10 mM glutathione. The GST fusion proteins of the intact and mutant 21st CCP domains were further purified on an Ni-NTA-agarose column. The purified proteins were dialyzed against 20 mM HEPES buffer (pH 8.0) containing 130 mM NaCl and quantified by the Bradford assay. A cDNA encoding the third fibronectin type III domain of human tenascin-C (TNfn3) was obtained by RT-PCR using RNA extracted from HT1080 cells and subcloned into pBluescript KS(+). A cDNA encoding human osteopontin was purchased from the National Institutes of Health Mammalian Gene Collection (Invitrogen), and a cDNA encoding the osteopontin N-terminal fragment (OPN-Nhalf) was amplified by PCR. The RGD motifs within TNfn3 and OPN-Nhalf were then mutated to RAA for specific binding to integrin α9β1 (referred to as TNfn3-RAA and OPN-Nhalf-RAA, respectively) (8, 33). After sequence verification, the cDNA fragments were inserted into pGEX4T-1 at the EcoRI/SalI sites. Both proteins were expressed and purified as described above.

Immunohistochemistry—Mouse embryos were embedded in OCT compound (Sakura Finetek, Tokyo, Japan) for cryosectioning. Sections (8–10-μm thickness) were fixed with 3.7% formaldehyde (single staining for polydom) or ice-cold acetone (double staining for polydom and integrin α9). The fixed sections were pretreated with chondroitinase ABC (5 units/ml) (Seikagaku Corp., Tokyo, Japan) and hyaluronidase (1 unit/ml) (Sigma) in PBS for 30 min at 37 °C, followed by inactivation of endogenous peroxidase with 0.3% H_2O_2 and blocking with PBS containing 1% BSA. The sections were labeled with antibodies overnight at 4 °C, and washed in PBS. The bound antibodies were visualized with HRP polymer-conjugated anti-rabbit IgG and 3,3′-diaminobenzidine (Dako, Glostrup, Denmark) or Alexa Fluor-conjugated secondary antibodies. Finally, the sections were counterstained with Mayer's hematoxylin (for 3,3′-diaminobenzidine staining) or Hoechst 33342 (for immunofluorescence staining) and mounted with Mount-Quick (Daido Sangyo, Tokyo, Japan) or fluorescent mounting medium (Dako).

In Situ Integrin Binding Assay—Frozen sections (8–10-μm thickness) of mouse embryos were fixed with ice-cold acetone for 15 min, washed with TBS, and blocked with 1% BSA in TBS. After three washes with TBS, the sections were incubated with recombinant integrin α9β1 (3 μg/ml) in TBS containing 1% BSA and 1 mM $MnCl_2$ at 4 °C overnight. The sections were then washed with TBS containing 1 mM $MnCl_2$ (TBS/Mn) and incubated with the anti-Velcro antibody (0.5 μg/ml) in TBS/Mn containing 1% BSA (TBS/Mn/BSA) for 2 h at room temperature. After washing with TBS/Mn, the sections were incubated with Alexa Fluor 488-conjugated goat anti-rabbit IgG in TBS/Mn/BSA for 2 h to visualize the bound anti-Velcro antibody. For double immunofluorescence staining with the anti-polydom or anti-tenascin-C antibody, sections were incubated with 100 μg/ml normal rabbit IgG (Dako) in TBS/Mn/BSA for 1 h to saturate the antigen-binding sites of the bound Alexa Fluor 488-conjugated goat anti-rabbit IgG. After washing with 20 mM

HEPES buffer (pH 7.5) containing 130 mM NaCl and 1 mM $MnCl_2$, the sections were refixed with 3.7% formaldehyde in 20 mM HEPES buffer (pH 7.5) containing 130 mM NaCl and 1 mM $MnCl_2$ for 10 min. The sections were then washed with TBS and incubated with Alexa Fluor 555-conjugated anti-pol-N antibody or the anti-tenascin-C antibody in TBS containing 1% BSA at 4 °C overnight. After washing in TBS, the bound anti-tenascin-C antibody was detected with Alexa Fluor 546-conjugated goat anti-rat IgG in TBS containing 1% BSA for 2 h. The sections were washed with TBS and mounted with fluorescent mounting medium (Dako).

RESULTS

Polydom Is an ECM Protein—Previously, we established a bioinformatics-based protocol for screening ECM proteins from transcriptome databases, and identified 16 new ECM proteins from >65,000 mouse cDNAs available in the RIKEN FANTOM cDNA collection (21). We extended this protocol to the Ensembl mouse and human genome databases to identify more ECM proteins by focusing on transcripts encoding proteins with >1500 amino acid residues. One of the obtained candidates was polydom (also named SVEP1), a putative secreted protein harboring EGF domains with strong similarities to those in the Notch family proteins (19, 20). Polydom comprises multiple domains characteristic of ECM proteins (*i.e.* a von Willebrand factor A domain, a pentraxin domain, 10 EGF-like domains, and 34 CCP (also called "sushi") domains) (19, 20) (Fig. 1*A*). To explore the biological functions of polydom, we amplified the cDNA encoding full-length mouse polydom by RT-PCR and expressed it in 293-F cells with a C-terminal FLAG tag. The recombinant polydom was detected in the culture medium and enriched by immunoprecipitation with an anti-FLAG antibody (Fig. 1*B*, *lane 1*), confirming that polydom is a secreted protein. However, the amount of the recombinant protein secreted into the medium was very low, yielding only a faint band on immunoblotting detection. To increase the expression level, recombinant polydom was expressed with a mouse immunoglobulin leader sequence and a C-terminal FLAG tag (Fig. 1*B*, *lane 2*) and purified from the spent medium by immunoaffinity chromatography using an anti-FLAG mAb. The purified recombinant polydom gave two major bands migrating at 250 and 100 kDa on SDS-PAGE under non-reducing conditions (Fig. 1*C*). Similar banding patterns were obtained under reducing conditions except that the two major bands migrated more slowly (270 and 115 kDa), suggesting that both were enriched in intrapeptide disulfide bonds. Determination of the N-terminal amino acid sequences of the two protein bands revealed that the 115 kDa band started with DAAQ, the putative N-terminal sequence after removal of the mouse immunoglobulin-derived leader sequence, whereas the 270 kDa band started with VAPG, which is identical to amino acids 1177–1180 located N-terminal to the first EGF domain (see Fig. 1*A*). These findings indicated that polydom was proteolytically processed, before or after secretion, into two parts (*i.e.* the N-terminal 115-kDa fragment and C-terminal 270-kDa fragment), which remained associated after the proteolytic cleavage.

To corroborate this conclusion, we expressed recombinant polydom with two tags, a FLAG tag at the N terminus and a His_6 tag at the C terminus, in 293-F cells and analyzed both the spent media and cell lysates by precipitation with anti-FLAG or Ni-NTA beads. Both the 270-kDa and 115-kDa fragments were recovered in the precipitates from the spent medium irrespective of the type of beads used (Fig. 1*D*), thereby confirming that these fragments remain associated. Notably, a high molecular weight band migrating in the >300 kDa region was detected in the precipitates from cell lysates with both the anti-FLAG and Ni-NTA beads. It therefore seems likely that the proteolytic processing into the N-terminal 115-kDa and C-terminal 270-kDa fragments occurs after secretion.

To examine whether polydom is an ECM protein, we produced antibodies against polydom and used them as immunohistochemical probes. Because polydom was cleaved into the N-terminal and C-terminal parts after secretion, we raised antibodies against recombinant full-length polydom in rabbits, followed by affinity purification of the antibodies using columns containing recombinant fragments for either amino acids 18–789 (designated pol-N) or amino acids 1192–3567 (designated pol-C) (see Fig. 1*A*). The specificities of these antibodies were verified by Western blotting using recombinant pol-N and pol-C fragments (Fig. 1*E*) as well as tissue extracts from E15.5 mouse embryo lungs (Fig. 1*F*). It should be noted that a higher molecular weight band migrating at the >300 kDa region was also detected by both the anti-pol-N and anti-pol-C antibodies in the tissue extracts, together with the N-terminally derived 90-kDa and C-terminally derived 250-kDa fragments (Fig. 1*F*, *arrowheads*), supporting the conclusion that polydom is proteolytically processed into two fragments both *in vivo* and *in vitro*. We used these antibodies for immunohistochemical staining of frozen sections of mouse embryos at E16.5 and obtained essentially the same results (Fig. 1*G* and supplemental Fig. S1). Polydom was detected in a variety of tissues, including the stomach, intestine, and lungs, where it was predominantly detected in the mesenchymal ECM. Polydom was also detected in the kidneys, liver, nerve fiber bundles, and choroid plexus (data not shown). Given the same staining patterns with the pol-N and pol-C antibodies, the N-terminal and C-terminal fragments appear to remain associated even after deposition in the ECM.

Polydom Mediates Integrin α9β1-dependent Cell Adhesion—To explore the biological functions of polydom, we examined whether it was capable of promoting cell adhesion using three human cell lines: A549 lung adenocarcinoma, HT1080 fibrosarcoma, and RD rhabdomyosarcoma. Although A549 and HT1080 cells failed adhere to polydom (data not shown), RD cells adhered to polydom in a coating concentration-dependent manner, attaining the maximum adhesion at 3 μg/ml (Fig. 2*A*). When the substrates were coated with either the recombinant pol-N or pol-C fragments, only the pol-C fragment was capable of promoting cell adhesion, with a potency that was almost equivalent to that of full-length polydom. The cells adhering to polydom and the pol-C fragment assumed spread morphology, although the extent of the spreading was less pronounced than that of cells adhering to fibronectin (Fig. 2*B*). These findings indicated that polydom is capable of mediating cell adhesion

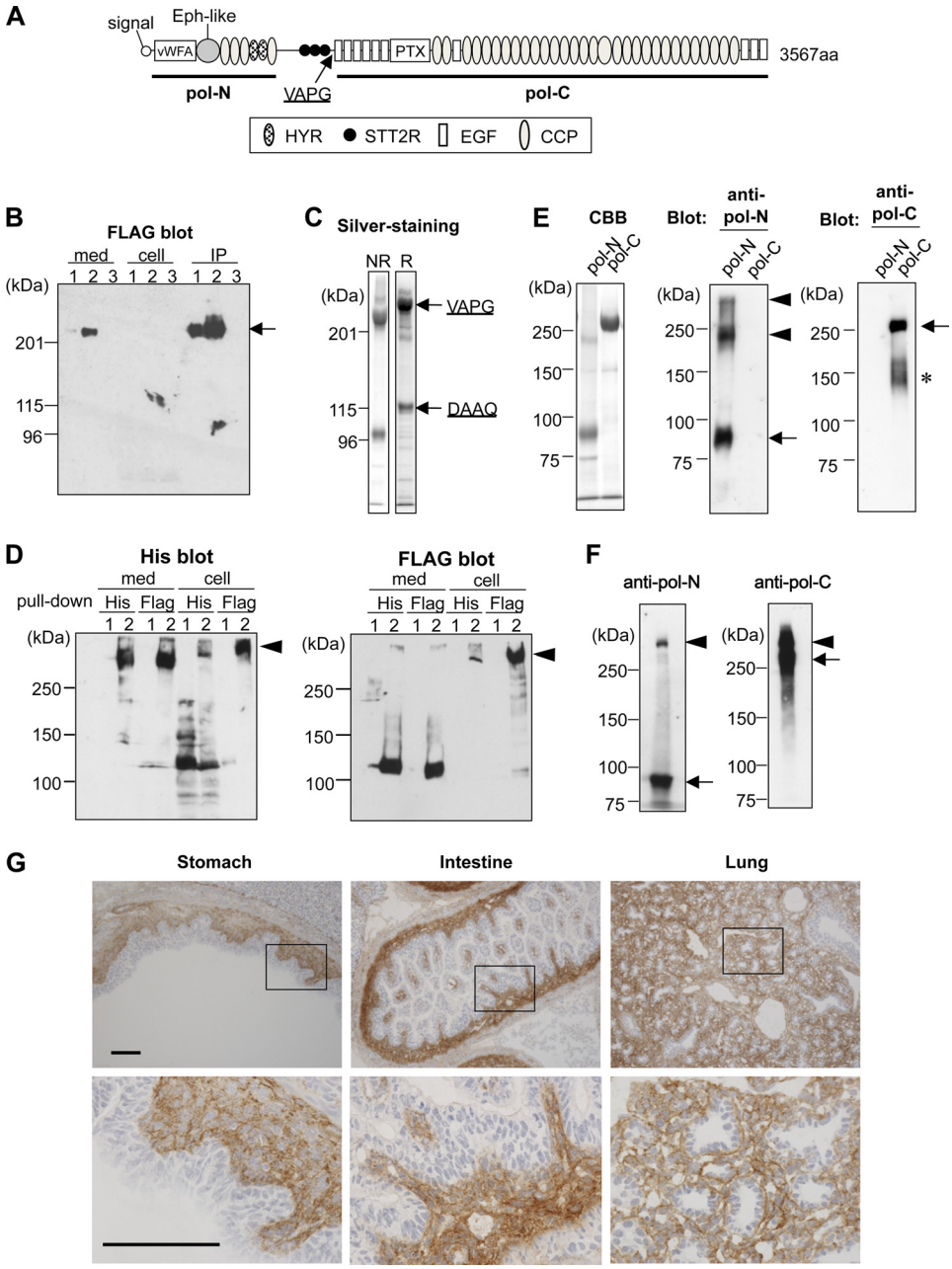

FIGURE 1. **Recombinant expression and immunohistochemical localization of polydom.** *A*, domain structure of mouse polydom. Polydom is a 3567-amino acid protein composed of an N-terminal signal sequence and an array of domains characteristic of ECM proteins. *vWFA*, von Willebrand factor type A domain; *Eph-like*, ephrin 2-like Cys-rich repeats; *HYR*, hyalin domain; *STT2R*, similar to thyroglobulin type 2 repeats; *EGF*, epithelial growth factor-like domain; *PTX*, pentraxin domain; *CCP*, complement control protein domain; *aa*, amino acid. The N-terminal and C-terminal regions represented by the recombinant pol-N and pol-C proteins are *underlined*. *B*, recombinant polydom with an N-terminal signal sequence of its own (*lane 1*) or a mouse immunoglobulin κ chain (*lane 2*) was expressed in 293-F cells with a C-terminal FLAG tag. The conditioned media (*med*), cell lysates (*cell*), and anti-FLAG immunoprecipitates from conditioned media (*IP*) were subjected to 6% SDS-PAGE under non-reducing conditions and subsequent immunoblotting with an HRP-conjugated anti-FLAG mAb. Untransfected 293-F cells were similarly processed in parallel (*lane 3*). *C*, affinity-purified FLAG-tagged polydom was subjected to 6% SDS-PAGE under non-reducing (*NR*) or reducing (*R*) conditions and subsequent silver staining. The N-terminal amino acid sequences determined by peptide sequencing are indicated on the *right*. *D*, recombinant polydom with both an N-terminal FLAG tag and a C-terminal His_6 tag was transfected into 293-F cells and then pulled down from culture media (*med*) and cell lysates (*cell*) using Ni-NTA (*His*) or anti-FLAG mAb-conjugated (*FLAG*) agarose. The precipitates were subjected to 5% SDS-PAGE under reducing conditions and analyzed by immunoblotting with anti-His (*left*) and anti-FLAG (*right*) mAbs. Untransfected (*lane 1*) and transfected (*lane 2*) cells were analyzed in parallel. Note that uncleaved polydom is detected in the cell lysates (*arrowheads*). *E*, recombinant pol-N or pol-C fragments were subjected to 6% SDS-PAGE under non-reducing conditions, followed by Coomassie Brilliant Blue staining (*left*) or immunoblotting with anti-pol-N (*middle*) and anti-pol-C (*right*) antibodies. Fragments at the 90 and 250 kDa regions were detected by the anti-pol-N and anti-pol-C antibodies, respectively (*arrows*). Oligomeric forms of the N-terminally derived fragment were also detected by the anti-pol-N antibody (*arrowheads*). Degradation products of the C-terminally derived fragment were also detected by the anti-pol-C antibody (*asterisk*). *F*, mouse E15.5 lung extracts (~100 μg of protein for the anti-pol-N antibody and ~35 μg of protein for the anti-pol-C antibody) were subjected to 5% SDS-PAGE under non-reducing conditions, followed by immunoblotting with the anti-pol-N (*left*) and anti-pol-C (*right*) antibodies. Both antibodies detected the >300-kDa full-length protein (*arrowheads*) as well as the 90-kDa (anti-pol-N) or 250-kDa (anti-pol-C) fragment (*arrows*). *G*, cryosections of mouse E16.5 embryos were stained with an anti-pol-N antibody. Representative images of the stomach, intestine, and lung are shown. The *bottom panels* show magnified views of the *boxed areas* in the *top panels*. *Bars*, 100 μm.

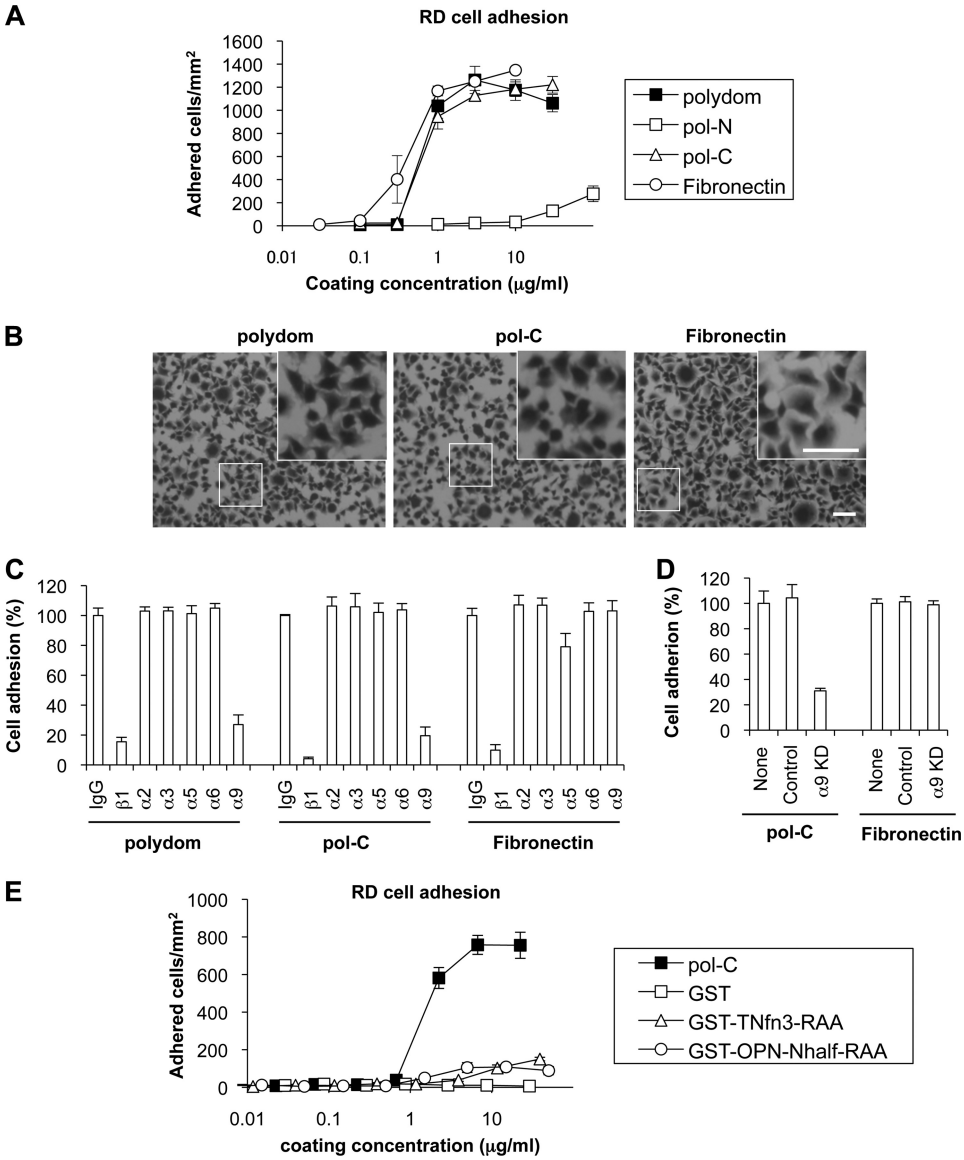

FIGURE 2. **Cell-adhesive activities of polydom.** *A*, RD cells were incubated at 37 °C for 30 min on 96-well microtiter plates coated with increasing concentrations of full-length polydom (*filled squares*), pol-N (*open squares*), pol-C (*open triangles*), or plasma fibronectin (*open circles*). After washing out unbound cells, the attached cells were fixed and stained with toluidine blue. The adhered cells were counted under a microscope. The data represent the means ± S.D. (*error bars*) of triplicate assays. *B*, photomicrographs of RD cells adherent on the substrates coated with full-length polydom (3 μg/ml), pol-C (3 μg/ml), or fibronectin (1 μg/ml). The *insets* show magnified views of the *boxed areas*. *Bar*, 60 μm. *C*, effects of anti-integrin mAbs on adhesion of RD cells to polydom. Ninety-six-well microtiter plates were coated with full-length polydom (3 μg/ml), pol-C (3 μg/ml), or plasma fibronectin (1 μg/ml). RD cells were preincubated with the following function-blocking mAbs at a concentration of 10 μg/ml for 10 min at room temperature before being added to the precoated wells: control mouse IgG (*IgG*), anti-integrin β1 mAb AIIB2 (*β1*), anti-integrin α2 mAb P1E6 (*α2*), anti-integrin α3 mAb 3G8 (*α3*), anti-integrin α5 mAb 8F1 (*α5*), anti-integrin α6 mAb AMCI7-4 (*α6*), and anti-integrin α9β1 mAb Y9A2 (*α9*). Unbound cells were washed out after 30 min of incubation at 37 °C, and the attached cells were fixed and stained with toluidine blue. The numbers of adherent cells are expressed as percentages of the numbers of adherent cells in the presence of control mouse IgG. The data represent the means ± S.D. of triplicate assays. The only partial inhibition by the anti-α5 mAb observed on fibronectin is caused by expression of integrin α4β1, another fibronectin-binding integrin, on RD cells (58). *D*, effects of integrin α9 knockdown on adhesion of RD cells to polydom. Ninety-six-well microtiter plates were coated with pol-C (3 μg/ml) or plasma fibronectin (1 μg/ml). Cells treated with the control siRNA (*Control*) or integrin α9 siRNA (*α9 KD*) were allowed to adhere on the plates for 30 min. The numbers of adherent cells are expressed as percentages of the numbers of adherent cells without siRNA treatment (*None*). The data represent the means ± S.D. of 5-well assays. *E*, RD cells were plated on 96-well microtiter plates coated with increasing concentrations of pol-C (*filled squares*), GST (*open squares*), GST-Tnfn3-RAA (*open triangles*), or GST-OPN-Nhalf-RAA (*open circles*) and incubated at 37 °C for 30 min. After washing out unbound cells, the attached cells were fixed, stained with toluidine blue, and counted under a microscope. The data represent the means ± S.D. of triplicate assays.

and subsequent cell spreading and that the cell adhesion-promoting activity resides within the C-terminal region composed of an array of CCP domains.

Next, we explored whether the adhesion of RD cells to polydom was dependent on integrins. The spread morphology of the cells adhering to polydom was indicative of the involvement of integrin-dependent cytoskeletal reorganization. In support of this possibility, the mAb against integrin β1 strongly inhibited the adhesion of RD cells to polydom. Among the mAbs against various integrin α subunits, the mAbs against integrins α2, α3, α5, and α6 did not inhibit cell adhesion to polydom, whereas the mAb against integrin α9β1 was strongly inhibitory

toward the RD cell adhesion to polydom (Fig. 2*C*). These findings are consistent with the failure of A549 and HT1080 cells to adhere to polydom because integrin α9β1 was expressed on RD cells (34) but not on A549 or HT1080 cells (supplemental Fig. S2*A*). Thus, it seems likely that the adhesion to polydom is primarily mediated by integrin α9β1.

To further investigate the role of integrin α9β1 in cell adhesion to polydom, we knocked down the expression of integrin α9 in RD cells by RNA interference. A significant reduction in the level of integrin α9 expression was verified by flow cytometric analysis (supplemental Fig. S2*B*). The siRNA-mediated integrin α9 knockdown resulted in an ~70% reduction in the number of cells adhering to pol-C, whereas cells treated with a control siRNA did not exhibit any significant decrease (Fig. 2*D*). The integrin α9 knockdown did not cause any reduction in cell adhesion to fibronectin, confirming that polydom is a specific ligand for integrin α9β1.

Because tenascin-C and osteopontin are well known ligands for integrin α9β1, we compared the cell adhesive activity of polydom with those of tenascin-C and osteopontin. Integrin α9β1 has been shown to bind to TNfn3 and the OPN-Nhalf (8, 9). We recombinantly expressed and purified these α9β1 ligands as GST fusion proteins, in which the RGD cell-adhesive motifs were replaced with RAA to nullify their abilities to interact with RGD-binding integrins, such as those containing the αV subunit (8, 33). RD cells adhered only poorly to GST-Tnfn3-RAA and GST-OPN-Nhalf-RAA, even at the highest coating concentration (*i.e.* >30 μg/ml), whereas the cells were fully competent in adhering to the recombinant pol-C fragment, attaining the maximum cell-adhesive activity at 7 μg/ml (Fig. 2*E*). These results indicate that polydom is more potent than tenascin-C and osteopontin as an integrin α9β1 ligand.

Polydom Is a Preferred Ligand for Integrin α9β1—To corroborate the role of integrin α9β1 as an adhesion receptor for polydom, we performed direct integrin binding assays using recombinant integrin α9β1, which was expressed and purified as a truncated disulfide-linked heterodimer with C-terminal FLAG (α9) and His_6 (β1) tags (31). The authenticity of the resulting integrin α9β1 was verified by SDS-PAGE and immunoblotting (Fig. 3, *A* and *B*). Solid-phase binding assays showed that the recombinant integrin α9β1 bound to full-length polydom and the pol-C fragment but not to the pol-N fragment (Fig. 3*C*). The binding of integrin α9β1 to polydom was completely abrogated in the presence of EDTA (Fig. 3*C*), thereby confirming the specificity of the integrin binding assays. Although cellular fibronectin containing the EIIIA domain is a putative ligand for integrin α9β1, recombinant integrin α9β1 exhibited only marginal binding activity toward recombinant cellular fibronectin, which was fully active in binding to integrin α5β1 (data not shown). These findings, together with those of the cell adhesion assays, corroborate the notion that integrin α9β1 binds directly to polydom, which has its integrin-binding site in the C-terminal 270-kDa region.

Next, we compared the integrin α9β1 binding activity of polydom with those of other known integrin α9β1 ligands (*i.e.* tenascin-C (TNfn3-RAA) and osteopontin (OPN-Nhalf-RAA)). Although TNfn3-RAA and OPN-Nhalf-RAA were capable of binding to integrin α9β1, their affinities for integrin

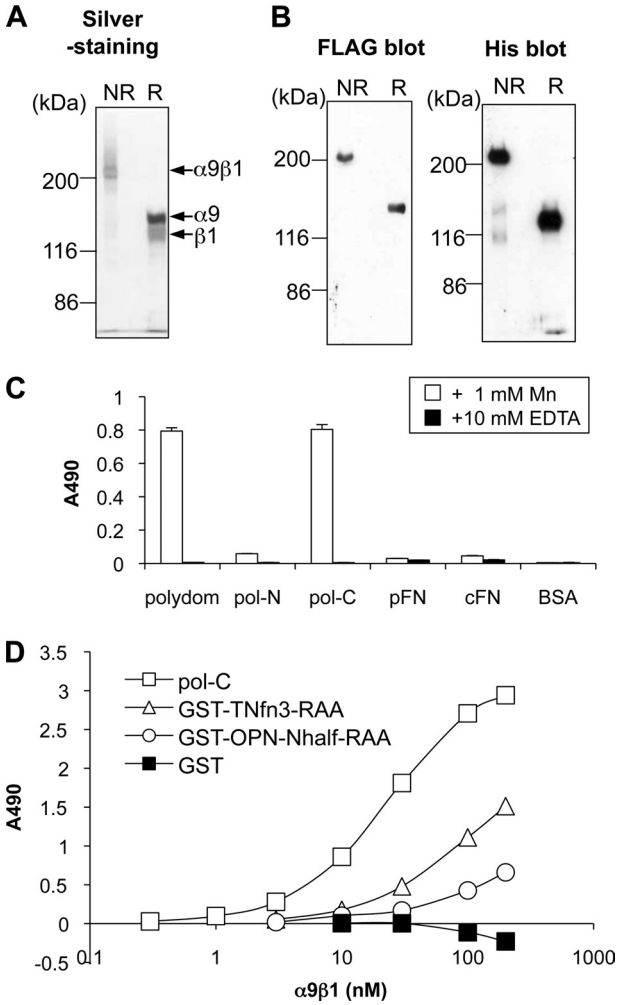

FIGURE 3. **Polydom binds to integrin α9β1 via its C-terminal region.** *A* and *B*, purified recombinant integrin α9β1 was subjected to 6% SDS-PAGE under non-reducing (*NR*) or reducing (*R*) conditions and visualized by silver staining (*A*) or immunoblotting with antibodies specific for the FLAG and His tags attached to the α9 and β1 chains, respectively (*B*). The positions of molecular weight markers are shown on the *left*. *C*, microtiter plates coated with 10 μg/ml full-length polydom, pol-N, pol-C, plasma fibronectin (*pFN*), cellular fibronectin (*cFN*), or BSA were incubated with recombinant integrin α9β1 in the presence of 1 mM $MnCl_2$ (*open bars*) or 10 mM EDTA (*filled bars*). The bound integrins were quantified using a biotinylated anti-Velcro antibody and HRP-conjugated streptavidin. The data represent the means ± S.D. (*error bars*) of triplicate determinations. *D*, titration curves of recombinant integrin α9β1 bound to polydom and other known α9β1 ligands. Integrin α9β1 at the indicated concentrations was allowed to bind to microtiter plates coated with pol-C (10 nM; *open squares*), GST-TNfn3-RAA (100 nM; *open triangles*), GST-OPN-Nhalf-RAA (100 nM; *open circles*), or GST (100 nM; *filled squares*) in the presence of 1 mM $MnCl_2$. The amounts of the integrin bound in the presence of 10 mM EDTA were taken as nonspecific binding and subtracted as background. The data represent the means of duplicate determinations.

α9β1 were significantly lower than that of pol-C (Fig. 3*D*). We were unable to determine the apparent dissociation constants for these α9β1 ligands due to incomplete saturation of binding at the highest integrin concentration, whereas the dissociation constant between integrin α9β1 and pol-C was estimated from three independent determinations to be 32.4 ± 2.7 nM. These results were consistent with those obtained by the cell adhesion assays and support the conclusion that polydom is a more potent ligand for integrin α9β1 than tenascin-C and osteopontin.

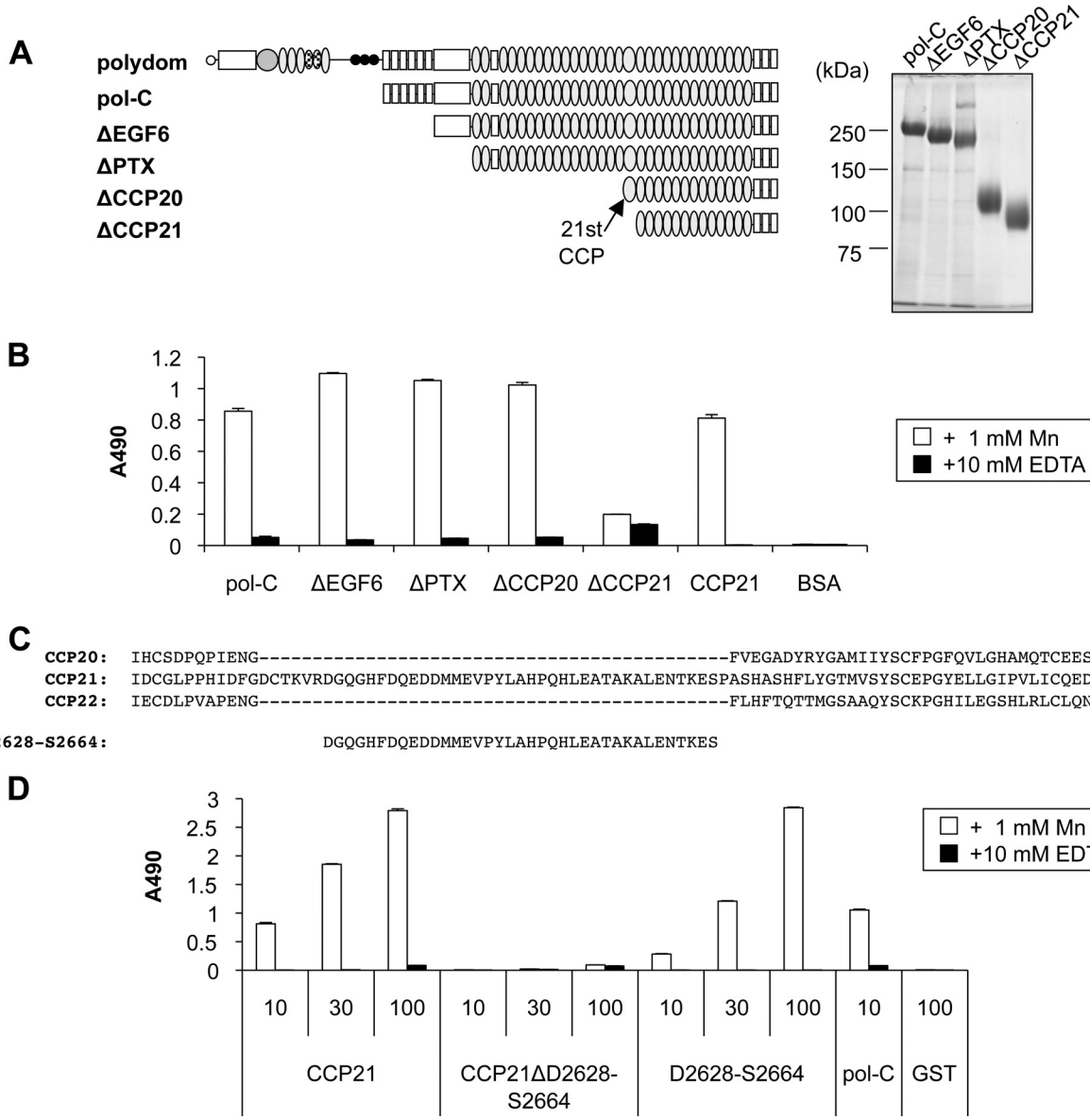

FIGURE 4. **Integrin α9β1 recognizes the 21st CCP domain.** *A*, a series of N-terminal deletion mutants of polydom (ΔEGF6, ΔPTX, ΔCCP20, and ΔCCP21) were produced. The purified mutant proteins were analyzed by 6% SDS-PAGE under non-reducing conditions and visualized by staining with Coomassie Brilliant Blue. The positions of molecular weight markers are shown on the *left*. *B*, recombinant proteins (10 nM) were coated on microtiter plates and assessed for their binding activities toward integrin α9β1 (10 nM) in the presence of 1 mM $MnCl_2$ (*open bars*) or 10 mM EDTA (*filled bars*). The data represent the means ± S.D. (*error bars*) of triplicate determinations. *C*, alignment of the amino acid sequences of the 21st CCP domain (*CCP21*) with its adjacent domains (*CCP20* and *CCP22*) by ClustalW. Different from the other CCP domains, CCP21 has an ~40-amino acid insertion. The 37-amino acid segment derived from the insert, Asp^{2628}–Ser^{2664} (*D2628-S2664*), was expressed as a GST fusion protein to assess the integrin α9β1 binding activities of the ~40-amino acid insert. *D*, integrin α9β1 (10 nM) was allowed to bind to microtiter plates coated with GST fusion proteins containing CCP21, CCP21 deleted of the 37-amino acid segment (*CCP21ΔD2628-S2664*), or the 37-amino acid segment alone (*D2628-S2664*) or with pol-C or GST alone at the indicated concentrations in the presence of 1 mM $MnCl_2$ (*open bars*) or 10 mM EDTA (*filled bars*). The results represent the means ± S.D. of triplicate determinations.

Integrin α9β1 Binds to the 21st CCP Domain—To locate the integrin α9β1-binding site within polydom, we constructed a series of N-terminal deletion mutants of pol-C (Fig. 4*A*) and examined their binding activities toward integrin α9β1. Although deletion up to the 20th CCP domain (designated ΔCCP20) did not compromise the integrin binding activity of pol-C, deletion of the 21st CCP domain (designated ΔCCP21) resulted in a dramatic loss of the activity (Fig. 4*B*), thereby underscoring the critical role of the 21st CCP domain (hereafter referred to as CCP21). To explore whether CCP21 harbors the integrin α9β1-binding site, we produced recombinant CCP21 as a GST fusion protein and examined its integrin α9β1 binding activity. CCP21 alone was fully active in binding to integrin α9β1 (Fig. 4*B*), confirming the critical role of CCP21 in the binding of polydom to integrin α9β1.

Among the 34 CCP domains within polydom, CCP21 is unique because it contains extra segment of ~40 amino acids compared with the other CCP domains (Fig. 4*C* and supplemental Fig. S3) (19). To examine whether the extra segment within CCP21 is involved in α9β1 binding, we deleted this segment (*i.e.* 37 amino acids encompassing Asp^{2628}–Ser^{2664}) from the GST-CCP21 fusion protein (designated ΔD2628-S2664; see

Fig. 4*C*). The resulting CCP21 mutant was unable to bind to integrin α9β1 (Fig. 4*D*), indicating the involvement of this extra segment in integrin α9β1 binding to CCP21. We also produced a GST fusion containing only the extra segment (Asp^{2628}–Ser^{2664}) and found that this extra segment retained the integrin binding activity of CCP21. These findings support the conclusion that the binding site for integrin α9β1 is located within the extra 37-amino acid segment of CCP21.

Integrin α9β1 Recognizes the Sequence EDDMMEVPY—To further narrow down the region responsible for α9β1 binding, we divided the extra 37-amino acid segment of CCP21 into N-terminal and C-terminal halves and determined their integrin binding activities (Fig. 5*A*). Integrin α9β1 only bound to the N-terminal segment Asp^{2628}–Leu^{2645}. We then divided the N-terminal segment into two partially overlapping segments, Asp^{2628}–Asp^{2638} and Asp^{2634}–Leu^{2645}. Only the C-terminally derived segment Asp^{2634}–Leu^{2645} was capable of binding to integrin α9β1 (Fig. 5*A*, *D2634-L2645*), showing that the binding site for integrin α9β1 could be mapped to the 12-amino acid segment DQEDDMMEVPYL within the extra segment of CCP21.

To identify the residues involved in binding to integrin α9β1, we performed alanine-scanning mutagenesis of the DQEDDMMEVPYL segment. Alanine substitution of Glu^{2641} almost completely abrogated the integrin binding activity, whereas mutations at the residues from Glu^{2636} to Tyr^{2644} caused partial reductions in the integrin binding activity to variable extents (Fig. 5*B*). These findings indicate that integrin α9β1 recognizes the EDDMMEVPY sequence, within which Glu^{2641} is the critical acidic residue involved in the polydom recognition by integrin α9β1.

To corroborate this conclusion, we produced two series of deletion mutants of the DQEDDMMEVPYL segment (*i.e.* those with N-terminal deletions and those with C-terminal deletions) (Fig. 5*C*). Integrin binding assays of the N-terminal deletion mutants revealed that deletion of Glu^{2636} and Asp^{2637} caused a small stepwise reduction in the integrin binding activity, whereas deletion of Asp^{2638} resulted in a dramatic loss of the activity. Similarly, deletion of Pro^{2643} and Val^{2642} from the C terminus of the DQEDDMMEVPYL segment caused a stepwise decrease in the integrin binding activity, although deletion of Tyr^{2644} did not. These findings were consistent with the conclusion that EDDMMEVPY is the recognition sequence for integrin α9β1, except that the involvement of Tyr^{2644} was not evident with the C-terminal deletion mutants.

To further corroborate the role of EDDMMEVPY as the integrin α9β1 recognition sequence, we performed the integrin inhibition assay with a synthetic EDDMMEVPY peptide. The EDDMMEVPY peptide inhibited the interaction of the pol-C fragment with integrin α9β1 in a dose-dependent manner, with an IC_{50} of 0.18 μM (Fig. 5*D*). A smaller peptide, DMMEVPY, was nearly as potent as EDDMMEVPY in inhibiting integrin α9β1 binding, consistent with the relatively small contribution of the N-terminal Glu-Asp residues to the interaction with integrin α9β1. Further deletion of the C-terminal Tyr residue from DMMEVPY resulted in a significant reduction in the inhibitory potency, supporting the involvement of Tyr^{2644} in the CCP21 recognition by integrin α9β1. Alanine substitution for Glu^{2641} in the DMMEVPY peptide resulted in a marked reduction of its inhibitory potency, consistent with the importance of Glu^{2641} in the recognition of polydom by integrin α9β1.

We also compared the inhibitory activity of the EDDMMEVPY peptide with those of the synthetic peptides AEIDGIEL and TYSSPEDGIHE, which represent the integrin α9β1 recognition sequences in tenascin-C and the fibronectin EIIIA domain, respectively (17, 35). AEIDGIEL was capable of inhibiting the integrin α9β1 binding to pol-C, although its potency was more than 1 order of magnitude less than that of EDDMMEVPY, with an IC_{50} of 7.8 μM (Fig. 5*D*). TYSSPEDGIHE was barely inhibitory toward the interaction between integrin α9β1 and pol-C. These findings support the conclusion that integrin α9β1 binds to polydom with an affinity that is significantly higher than those to tenascin-C and that EDDMMEVPY is a preferred sequence for ligand recognition by integrin α9β1.

Polydom Partially Colocalizes with Integrin α9 in Tissues—The relatively high binding affinity of polydom toward integrin α9β1 suggests that polydom functions as a physiological ligand of integrin α9β1. To address this possibility, we performed immunofluorescence staining of mouse embryonic tissues with antibodies against polydom and integrin α9. Polydom was colocalized with integrin α9 at the submucosal mesenchyme in the stomach and intestine (Fig. 6, *A–F*). Integrin α9 was also expressed in the smooth muscle layer in these tissues, where polydom was barely expressed. Polydom and integrin α9 were also colocalized at the sinusoids in the liver (Fig. 6, *G–I*) and Bowman's capsules (*arrowheads*) and the mesenchyme between renal tubules (*arrows*) in the kidney (Fig. 6, *J–L*). In the lung, polydom was detected in the mesenchyme, where integrin α9 was only partially colocalized (Fig. 6, *M–O*). Integrin α9 was strongly expressed in the smooth muscle layer of the lung, where polydom was barely detectable. These findings demonstrated that polydom was colocalized with integrin α9 in the embryonic mesenchyme of various organs, except for the smooth muscle layers where integrin α9 was highly expressed, consistent with the possibility that polydom serves as one of the physiological ligands of integrin α9β1.

To further corroborate the role of polydom as a physiological ligand for integrin α9β1, we performed *in situ* integrin overlay assays to visualize the integrin α9β1 ligands in tissues as a whole. Incubation of frozen tissue sections of mouse embryos with recombinant integrin α9β1 detected its ligands in the mesenchyme and smooth muscle layer of the stomach, intestine, and lung when the incubation was carried out in the presence of Mn^{2+} (Fig. 7, *A*, *E*, and *I*). No signals were detected when the assay was performed in the presence of EDTA (Fig. 7, *D*, *H*, and *L*), confirming the specificity of the *in situ* integrin overlay assay. Double immunofluorescence detection of polydom using an Alexa Fluor 555-conjugated anti-polydom antibody demonstrated that the signals for polydom overlapped with those for bound integrin α9β1 in the mesenchymal region of the stomach, intestine, and lung (Fig. 7, *C*, *G*, and *K*). We also performed double immunofluorescence detection using an anti-tenascin-C antibody (supplemental Fig. S4). The signals for tenascin-C overlapped with those for bound integrin α9β1 in the smooth muscle layer of the stomach and part of the mesen-

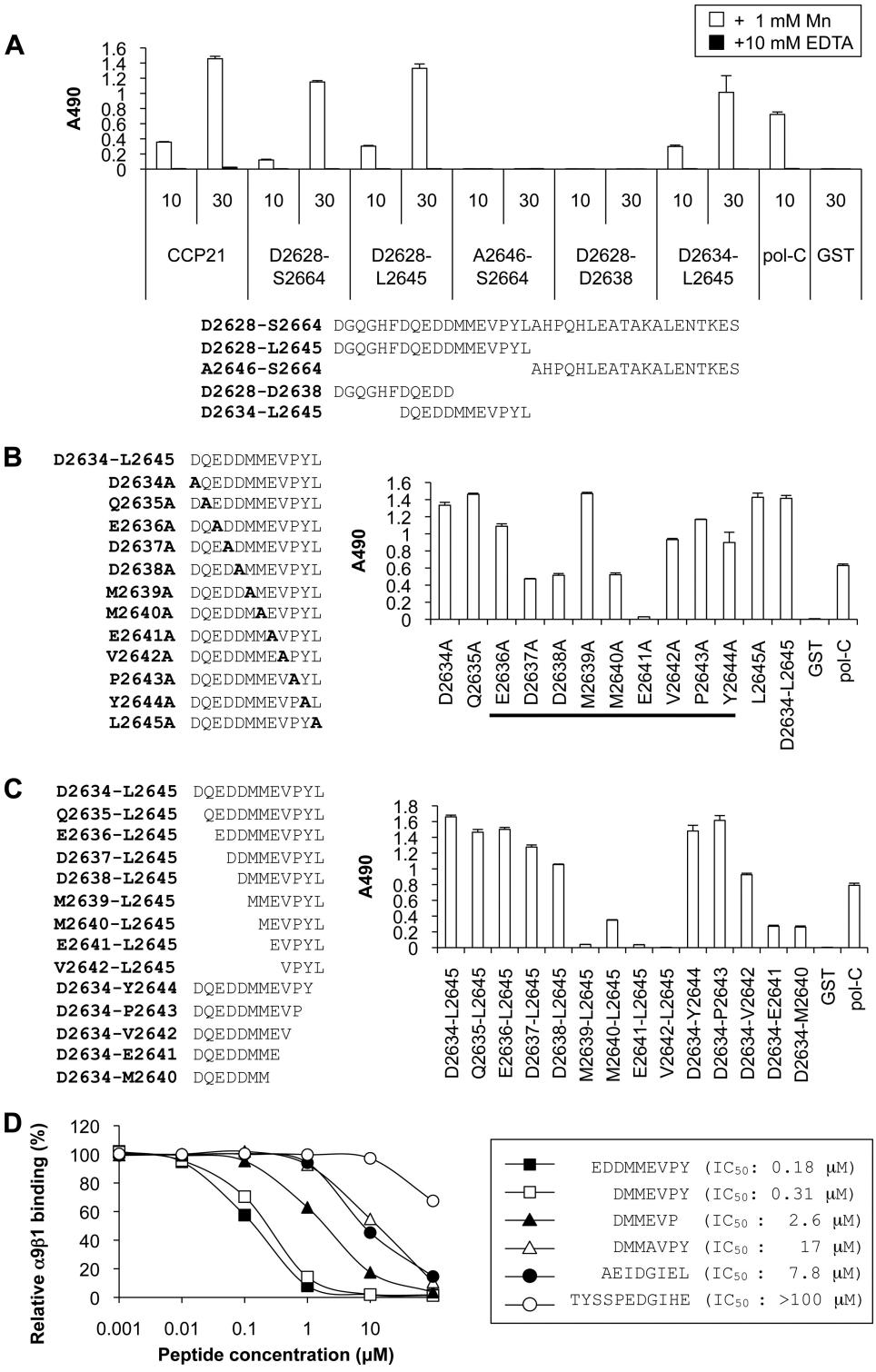

FIGURE 5. **Identification of the amino acid residues in CCP21 involved in binding to integrin α9β1.** *A*, the 37-amino acid segment was divided into a series of smaller segments and expressed as GST fusion proteins. The resulting GST fusion proteins, together with pol-C and GST alone, were coated on microtiter plates at 10 or 30 nM and subjected to integrin α9β1 binding assays in the presence of 1 mM $MnCl_2$ (*open bars*) or 10 mM EDTA (*filled bars*). The bound integrins were quantified. The data represent the means ± S.D. (*error bars*) of triplicate determinations. *B* and *C*, the integrin α9β1 binding activities of the alanine scanning mutants (*B*) and N-terminal or C-terminal deletion mutants (*C*) of the Asp^{2634}–Leu^{2645} (*D2634-L2645*) segment. GST fusion proteins containing the mutated segments (30 nM) were coated onto microtiter plates and subjected to integrin α9β1 binding assays. The bound integrins were quantified. The data represent the means ± S.D. of triplicate determinations. *D*, inhibition of integrin α9β1 binding to pol-C by synthetic peptides. Integrin α9β1 (10 nM) was incubated on microtiter plates coated with pol-C (10 nM) in the presence of 1 mM $MnCl_2$ and increasing concentrations of synthetic peptides. To prevent precipitation of the peptides, the integrin binding assays were performed in the presence of 10% dimethyl sulfoxide. The amounts of bound integrin α9β1 are expressed as percentages relative to the control, in which integrin α9β1 was incubated on pol-C-coated plates in the absence of peptides. The results represent the means of duplicate determinations. The IC_{50} values of the peptides are shown in the *right panel*.

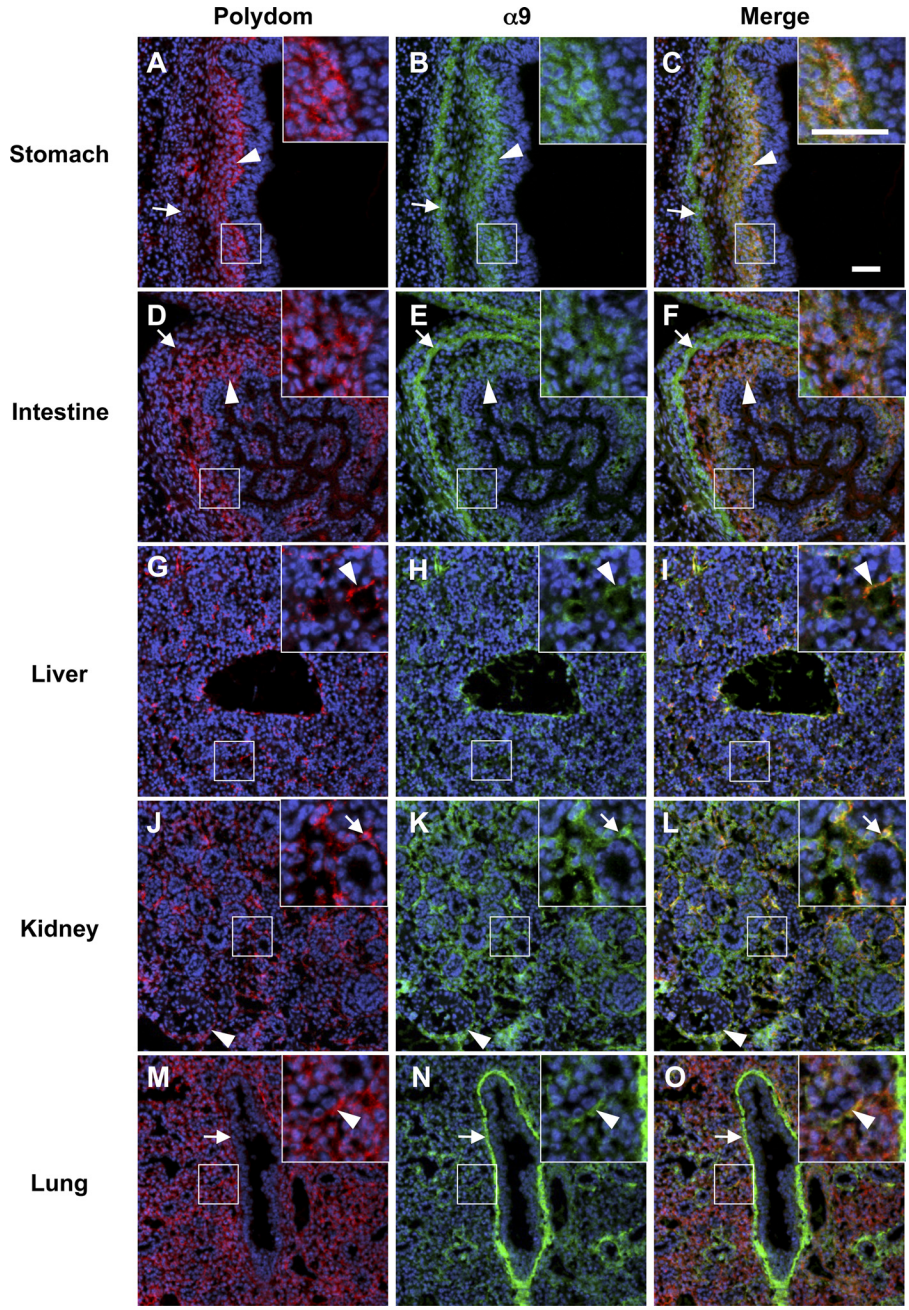

FIGURE 6. **Immunofluorescence localization of polydom and integrin α9.** *A–O*, cryosections of mouse E16.5 embryos were labeled with antibodies against polydom (*anti-pol-N* (*red*); *A*, *D*, *G*, *J*, and *M*) and integrin α9 (*green*; *B*, *E*, *H*, *K*, and *N*). *Merged images* are shown in the *right panels* (*C*, *F*, *I*, *L*, and *O*). Nuclei were stained with Hoechst 33342 (*blue*). Representative images of the stomach (*A–C*), intestine (*D–F*), liver (*G–I*), kidney (*J–L*), and lung (*M–O*) are shown. The *insets* are magnified views of the *boxed areas*. *Bar*, 50 μm.

chyme in the lung, although tenascin-C was not detected in the submucosal mesenchyme in the stomach, where signals for polydom and bound integrin α9β1 were colocalized (Fig. 7*C*). Given the potent binding affinity of polydom toward integrin α9β1, these results support the possibility that polydom functions as a physiological ligand for integrin α9β1, complementing tenascin-C and other known integrin α9β1 ligands. It should also be noted that strong signals for bound integrin α9β1 were detected in the smooth muscle layer surrounding the trachea, where polydom and tenascin-C were barely expressed (*arrows* in Fig. 7*K* and supplemental Fig. S4*F*), indicating the presence of one or more other ligands for integrin α9β1 in these regions.

DISCUSSION

In the present study, we obtained evidence that polydom is an ECM protein that functions as a ligand for integrin α9β1. Polydom was secreted into the culture media when transfected into 293-F cells. Deposition to the ECM *in vivo* was demonstrated by immunohistochemistry. Polydom was capable of mediating cell-to-substrate adhesion of RD cells that express integrin α9 but not of A549 or HT1080 cells that do not express

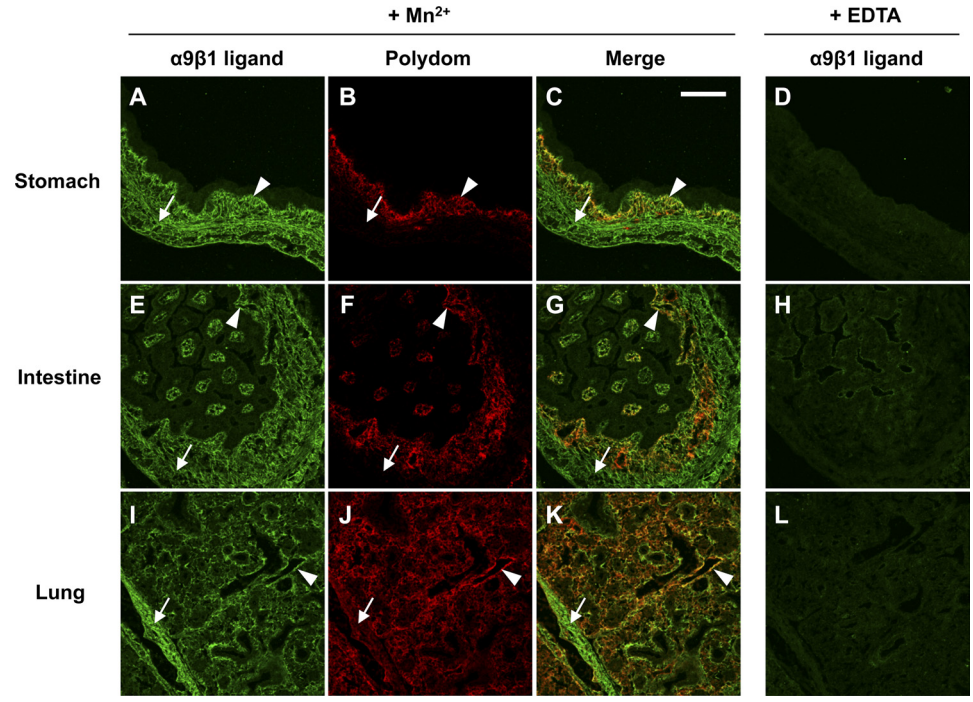

FIGURE 7. **Detection of integrin α9β1 ligands in tissues.** *A–L*, cryosections of mouse E16.5 embryos were incubated with recombinant integrin α9β1 in the presence of 1 mM $MnCl_2$ (*A–C*, *E–G*, and *I–K*) or 10 mM EDTA (*D*, *H*, and *L*) together with an Alexa Fluor 555-conjugated anti-pol-N antibody (*B*, *F*, and *J*). *Merged images* (*C*, *G*, and *K*) are also shown. Representative images of the stomach (*A–D*), intestine (*E–H*), and lung (*I–L*) are shown. The integrin α9β1 signals are almost completely lost upon incubation in the presence of 10 mM EDTA. The integrin signals are partially colocalized with those of polydom (*arrowheads*). Note that the smooth muscle layers are positive for integrin α9β1 ligands but negative for polydom (*arrows*). *Bar*, 100 μm.

integrin α9. The adhesion of RD cells to polydom was specifically inhibited by treatment of the cells with anti-integrin α9β1 antibodies and by siRNA-mediated knockdown of integrin α9, indicating that the cell adhesion to polydom was integrin α9β1-dependent. In support of the conclusion, recombinant integrin α9β1 bound to polydom in a divalent metal ion-dependent manner with an affinity that was significantly greater than those to tenascin-C and osteopontin, which are two well known ECM ligands for integrin α9β1. Polydom was partially colocalized with integrin α9 in mouse embryonic tissues. Furthermore, the *in situ* integrin overlay assay, which visualizes the entire ligands available for a given integrin overlaid on tissue sections, demonstrated that the immunohistochemical signals for polydom significantly overlapped with those obtained by the integrin α9β1 overlay. Taken together, these findings led us to conclude that polydom is an ECM protein that functions as a ligand for integrin α9β1 *in vivo*.

To date, a number of proteins have been shown to bind to integrin α9β1. These include tenascin-C, osteopontin, the EIIIA domain of fibronectin, ADAMs, and VEGF (8–10, 13, 16, 17, 35–39). Among these, tenascin-C, and particularly its third fibronectin type III domain (TNfn3), has been used as a representative for integrin α9β1 ligands. Our results showed that polydom bound to integrin α9β1 with higher affinity than TNfn3, with a dissociation constant of 32.4 ± 2.7 nM. This dissociation constant is comparable with those for the interactions of integrin α6β4 with laminin-332 (12 ± 3 nM) and laminin-511/521 (25 ± 1 nM) (31), suggesting that polydom is a more preferred physiological ligand for integrin α9β1 than tenascin-C. Indeed, polydom can explain, at least in part, the integrin α9β1 ligands detected by the *in situ* integrin α9β1 overlay assay in the submucosal mesenchyme of the developing gastrointestinal tract. It should be noted, however, that polydom cannot explain the integrin α9β1 ligands in the smooth muscle layers in the stomach, intestine, and lung, where polydom was barely expressed. Recently, EMILIN-1 has been shown to be a ligand for integrin α9β1 (40). Because EMILIN-1 is highly expressed in smooth muscle cells (41), it may account for the major integrin α9β1 ligands in these smooth muscle layers. It remains to be determined whether EMILIN-1 binds to integrin α9β1 with an affinity that is comparable with that of polydom.

The peptide sequences recognized by integrin α9β1 have been reported for a number of integrin α9β1 ligands. These sequences include AEIDGIEL in TNfn3 (35) and TYSSPEDGIHE in the EIIIA domain of fibronectin (17). In the present study, we found that EDDMMEVPY is the polydom sequence recognized by integrin α9β1. This conclusion was drawn from the integrin α9β1 binding assays using a series of alanine substitution as well as N-terminal and C-terminal deletion mutants of CCP21, which harbors the integrin α9β1 binding activity of polydom. The importance of the EDDMMEVPY sequence for binding to integrin α9β1 was further confirmed by integrin binding inhibition assays with a synthetic EDDMMEVPY peptide, which exhibited a potent inhibitory activity with an IC_{50} of 0.18 μM, whereas AEIDGIEL and TYSSPEDGIHE were about >10-fold and >100-fold less potent than EDDMMEVPY.

In the EDDMMEVPY sequence, the sixth Glu residue (Glu^{2641}) is critical for integrin α9β1 binding, because alanine substitution of this residue completely abolished the integrin α9β1 binding activity of CCP21. Consistent with this conclusion, the DMMAVPY peptide, in which alanine was substituted

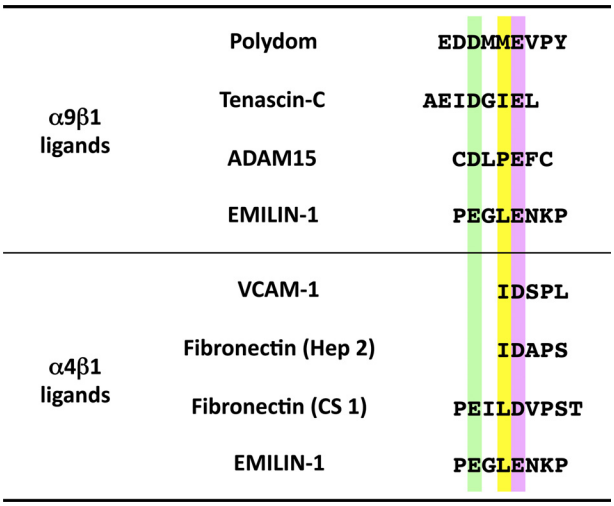

FIGURE 8. **Alignment of the recognition sequences for integrins α4β1 and α9β1.** The recognition sequences for integrin α9β1 (*i.e.* polydom and tenascin-C (35), ADAM15 (11), and EMILIN-1 (40)) and integrin α4β1 (VCAM-1 (47), fibronectin heparin-binding domain 2 (48), fibronectin type III CS1 (59), and EMILIN-1 (38)) were aligned to highlight the consensus (E/D)*X*Φ(E/D) motif, where Φ indicates a hydrophobic residue. The first E/D, hydrophobic, and second E/D residues are highlighted in *green*, *yellow*, and *pink*, respectively.

for Glu^{2641}, was >50-fold less potent than the control DMMEVPY peptide in inhibiting the interaction between integrin α9β1 and polydom. It is known that integrin ligands contain a critical acidic residue for their interactions with integrins (42–44). Accumulating evidence indicates that the carboxyl group of the acidic residue coordinates the divalent metal ion in the so-called metal ion-dependent adhesion site (MIDAS), thereby securing the binding to integrins (45). It therefore seems likely that Glu^{2641} is the acidic residue that coordinates the metal ion in the MIDAS of the integrin β1 chain. However, one may argue against this conclusion because deletion of this Glu residue from the DQEDDMME peptide did not cause a further reduction in the integrin binding activity (Fig. 5*C*). A possible explanation for the apparent discrepancy would be that the α-carboxyl group of the C-terminal methionine residue of the resulting DQEDDMM peptide may play a role that is functionally equivalent to the side chain of Glu^{2641} in coordinating the metal ion in the MIDAS. In support of this possibility, the crystal structure of integrin αIIbβ3 complexed with the peptide derived from the C-terminal region of the γ subunit of fibrinogen, referred to as the γC peptide, revealed that the free α-carboxyl group of the C-terminal residue of the γC peptide coordinates the divalent metal cation at the "adjacent to MIDAS" (ADMIDAS) region of integrin β3 (46). Thus, the free α-carboxyl group of the C-terminal methionine residue of the DQEDDMM peptide may coordinate the divalent metal ion at the MIDAS or ADMIDAS of the β1 subunit of integrin α9β1 and thereby partially substitute for the side chain of Glu^{2641} to stabilize the binding of integrin α9β1 to the truncated peptide.

It is interesting to note that most, if not all, of the sequences reported as integrin α9β1 recognition sites contain a hydrophobic residue that precedes the acidic residue critical for binding to the integrin (Fig. 8). Furthermore, another acidic residue is often situated two residues N-terminal to the hydrophobic residue, as has been shown for the proposed α9β1 recognition sequences of tenascin-C (AEIDGIEL) and ADAM-15 (DLPEF) (11, 35). The D*XX*E motif is well conserved among the ~30 members of the ADAM family proteases, except for ADAM-10 and ADAM-17, which both lack integrin α9β1-dependent cell-adhesive activity (11). Given that the EDDMMEVPY sequence in polydom also agrees with this rule, the D*X*ΦE motif (where Φ represents a hydrophobic residue) seems to be the preferred sequence recognized by integrin α9β1 (Fig. 8). Interestingly, a motif similar to D*X*ΦE is also found in the ligands recognized by integrin α4β1 (44, 47) (*i.e.* fibronectin (PEILDVPST) and EMILIN-1 (PEGLENKP, the latter of which was recently shown to bind to integrin α9β1 as well) (40). Consistent with this similarity between integrins α4β1 and α9β1 in their recognition sequences, integrin α4 exhibits the highest sequence homology with integrin α9 among the 18 integrin α subunits (2). Other integrin α4β1 ligands contain a Φ(E/D) motif in their integrin recognition sequences, including IDSP in VCAM-1 (47) and IDAP in the C-terminal heparin-binding domain of fibronectin (48), underscoring the importance of the hydrophobic residue preceding the critical acidic residue in ligand recognition by integrins α4β1 and α9β1 (Fig. 8).

Although the coordination of the carboxyl group of an acidic residue with the divalent metal ion in the MIDAS is critical for ligand binding to integrins, additional interactions between residues in the integrin headpiece and those in the integrin recognition sequence of the ligand are required to secure the ligand binding to integrins. The crystal structure of integrin αVβ3 complexed with an RGD-containing ligand revealed that the side chain of the Arg residue in the RGD motif formed salt bridges to two Asp residues in the β-propeller domain of the integrin αV subunit (49). Interestingly, the two Asp residues in integrin αV are replaced by Lys or Arg residues in integrins α4 and α9, and these basic residues are well conserved within vertebrates (supplemental Fig. S5). By analogy with the RGD recognition by integrin αvβ3, it is tempting to speculate that these basic residues in integrins α4 and α9 may form salt bridges with the most N-terminal acidic residue in the (E/D)*X*Φ(E/D) motif, whereas the critical acidic residue coordinates the divalent metal ion in the MIDAS. Thus, the N-terminal three acidic residues of the EDDMMEVPY motif in polydom may well be engaged in forming salt bridges with the basic residues in the β-propeller domain of integrin α9.

Polydom is a large modular protein containing a von Willebrand factor A domain, a pentraxin domain, EGF-like domains and an array of CCP domains. Genes encoding its homologues with similar domain compositions and alignments have been found in both vertebrates and invertebrates, including honey bees, mosquitoes, sea urchins, fish, mice, rats, dogs, and monkeys (50). Thus, polydom is an evolutionarily conserved protein with function(s) shared among metazoans. It should be noted, however, that long arrays of CCP domains, including the one containing the D*X*ΦE motif, are absent from invertebrates. Furthermore, the EDDMMEVPY sequence in the extra region of CCP21 is only conserved in mammals (supplemental Fig. S6). It seems likely that the ability to interact with integrin α9β1 was acquired in a later stage of evolution and was not the prototypical function of polydom. Consistent with this

possibility, integrin α9 homologues are found only in vertebrates (51). Given that the N-terminal half comprising a von Willebrand factor A domain, a pentraxin domain, EGF-like domains, and a stretch of a few CCP domains is conserved in both vertebrates and invertebrates, this region should have another function, other than binding to integrin α9β1, that remains to be explored to understand the physiological roles of polydom in metazoans.

Integrins transduce signals into cells upon binding with their ligands, thereby regulating cell proliferation, morphology, and migration (52, 53). Despite a plethora of information on the signaling events triggered by RGD-binding or laminin-binding integrins (54, 55), there is only limited information regarding those triggered by integrin α9β1, partly because of the limited availability of cells expressing high levels of the integrin and also because of the difficulties in analyzing integrin-mediated signals on low affinity ligands. Gupta and Vlahakis (34) reported that integrin α9β1-dependent cell adhesion to TNfn3-RAA not only activates c-Src kinase with concomitant tyrosine phosphorylation of $p130^{Cas}$ and activation of Rac-1, both of which are well known signaling events triggered by a variety of integrins, including integrins α3β1 and α5β1 (55, 56), but also enhances nitric oxide production through activation of inducible nitric-oxide synthase, which is so far unique to the signaling events triggered by integrin α9β1. Furthermore, Sheppard *et al.* (57) demonstrated that integrin α9β1 binds to spermidine/spermine-N^1-acetyltransferase via the cytoplasmic domain of integrin α9 and enhances cell migration by modulating the local concentration of spermidine/spermine, which in turn regulates the K^+ ion efflux by blocking inward rectifier K^+ channels. Thus, integrin α9β1 may trigger both signaling pathways, one common to other integrins and the other unique to integrin α9β1. In this respect, cells cultured in the presence of an EMILIN-1 fragment exhibited reduced cell proliferation in an integrin α9β1-dependent manner (40), raising the possibility that, unlike other integrins, integrin α9β1 elicits signals that suppress, but do not accelerate, cell cycle progression. Currently, the mechanism by which integrin α9β1 negatively regulates cell proliferation remains only poorly understood. Given its high binding affinity toward integrin α9β1, polydom represents an excellent adhesive ligand for analyzing the signaling pathways activated by ligation of integrin α9β1 and should contribute to uncovering the hitherto unknown physiological functions of integrin α9β1 in diverse biological processes, including cell migration, cell proliferation, wound healing, lymphangiogenesis, and hematopoietic homeostasis, in which integrin α9β1 has been implicated.

Acknowledgments—We thank Dr. Junichi Takagi (Institute for Protein Research, Osaka University, Japan) for the expression vector for integrin β1 with a His_6 tag, Dr. Masahiko Katayama (Eisai Co., Ltd., Tsukuba, Japan) for providing the mAb against integrin α6 (AMCI7–4), and Dr. Naoko Norioka (Institute for Protein Research, Osaka University, Japan) for the N-terminal amino acid sequence analyses. The bioinformatics-based screening for ECM proteins was performed using the computer system of the Genome Information Research Center, Research Institute for Microbial Diseases, Osaka University.

REFERENCES

1. Humphries, M. J. (2002) Insights into integrin-ligand binding and activation from the first crystal structure. *Arthritis Res.* **4,** 69–78
2. Palmer, E. L., Rüegg, C., Ferrando, R., Pytela, R., and Sheppard, D. (1993) Sequence and tissue distribution of the integrin α9 subunit, a novel partner of β1 that is widely distributed in epithelia and muscle. *J. Cell Biol.* **123,** 1289–1297
3. Wang, A., Patrone, L., McDonald, J. A., and Sheppard, D. (1995) Expression of the integrin subunit α9 in the murine embryo. *Dev. Dyn.* **204,** 421–431
4. Stepp, M. A., Zhu, L., Sheppard, D., and Cranfill, R. L. (1995) Localized distribution of α9 integrin in the cornea and changes in expression during corneal epithelial cell differentiation. *J. Histochem. Cytochem.* **43,** 353–362
5. Huang, X. Z., Wu, J. F., Ferrando, R., Lee, J. H., Wang, Y. L., Farese, R. V., Jr., and Sheppard, D. (2000) Fatal bilateral chylothorax in mice lacking the integrin α9β1. *Mol. Cell Biol.* **20,** 5208–5215
6. Bazigou, E., Xie, S., Chen, C., Weston, A., Miura, N., Sorokin, L., Adams, R., Muro, A. F., Sheppard, D., and Makinen, T. (2009) Integrin-α9 is required for fibronectin matrix assembly during lymphatic valve morphogenesis. *Dev. Cell* **17,** 175–186
7. Singh, P., Chen, C., Pal-Ghosh, S., Stepp, M. A., Sheppard, D., and Van De Water, L. (2009) Loss of integrin α9β1 results in defects in proliferation, causing poor re-epithelialization during cutaneous wound healing. *J. Invest. Dermatol.* **129,** 217–228
8. Yokosaki, Y., Palmer, E. L., Prieto, A. L., Crossin, K. L., Bourdon, M. A., Pytela, R., and Sheppard, D. (1994) The integrin α9β1 mediates cell attachment to a non-RGD site in the third fibronectin type III repeat of tenascin. *J. Biol. Chem.* **269,** 26691–26696
9. Smith, L. L., Cheung, H. K., Ling, L. E., Chen, J., Sheppard, D., Pytela, R., and Giachelli, C. M. (1996) Osteopontin *N*-terminal domain contains a cryptic adhesive sequence recognized by α9β1 integrin. *J. Biol. Chem.* **271,** 28485–28491
10. Liao, Y. F., Gotwals, P. J., Koteliansky, V. E., Sheppard, D., and Van De Water, L. (2002) The EIIIA segment of fibronectin is a ligand for integrins α9β1 and α4β1, providing a novel mechanism for regulating cell adhesion by alternative splicing. *J. Biol. Chem.* **277,** 14467–14474
11. Eto, K., Huet, C., Tarui, T., Kupriyanov, S., Liu, H. Z., Puzon-McLaughlin, W., Zhang, X. P., Sheppard, D., Engvall, E., and Takada, Y. (2002) Functional classification of ADAMs based on a conserved motif for binding to integrin α9β1. Implications for sperm-egg binding and other cell interactions. *J. Biol. Chem.* **277,** 17804–17810
12. Taooka, Y., Chen, J., Yednock, T., and Sheppard, D. (1999) The integrin α9β1 mediates adhesion to activated endothelial cells and transendothelial neutrophil migration through interaction with vascular cell adhesion molecule-1. *J. Cell Biol.* **145,** 413–420
13. Vlahakis, N. E., Young, B. A., Atakilit, A., and Sheppard, D. (2005) The lymphangiogenic vascular endothelial growth factors VEGF-C and -D are ligands for the integrin α9β1. *J. Biol. Chem.* **280,** 4544–4552
14. Staniszewska, I., Sariyer, I. K., Lecht, S., Brown, M. C., Walsh, E. M., Tuszynski, G. P., Safak, M., Lazarovici, P., and Marcinkiewicz, C. (2008) Integrin α9β1 is a receptor for nerve growth factor and other neurotrophins. *J. Cell Sci.* **121,** 504–513
15. Smith, L. L., and Giachelli, C. M. (1998) Structural requirements for α9β1-mediated adhesion and migration to thrombin-cleaved osteopontin. *Exp. Cell Res.* **242,** 351–360
16. Nishimichi, N., Higashikawa, F., Kinoh, H. H., Tateishi, Y., Matsuda, H., and Yokosaki, Y. (2009) Polymeric osteopontin employs integrin α9β1 as a receptor and attracts neutrophils by presenting a *de novo* binding site. *J. Biol. Chem.* **284,** 14769–14776
17. Shinde, A. V., Bystroff, C., Wang, C., Vogelezang, M. G., Vincent, P. A., Hynes, R. O., and Van De Water, L. (2008) Identification of the peptide sequences within the EIIIA (EDA) segment of fibronectin that mediate integrin α9β1-dependent cellular activities. *J. Biol. Chem.* **283,** 2858–2870
18. Bazan-Socha, S., Kisiel, D. G., Young, B., Theakston, R. D., Calvete, J. J., Sheppard, D., and Marcinkiewicz, C. (2004) Structural requirements of MLD-containing disintegrins for functional interaction with α4β1 and

α9β1 integrins. *Biochemistry* **43,** 1639–1647
19. Gilgès, D., Vinit, M. A., Callebaut, I., Coulombel, L., Cacheux, V., Romeo, P. H., and Vigon, I. (2000) Polydom. A secreted protein with pentraxin, complement control protein, epidermal growth factor, and von Willebrand factor A domains. *Biochem. J.* **352,** 49–59
20. Shur, I., Socher, R., Hameiri, M., Fried, A., and Benayahu, D. (2006) Molecular and cellular characterization of SEL-OB/SVEP1 in osteogenic cells *in vivo* and *in vitro*. *J. Cell Physiol.* **206,** 420–427
21. Manabe, R., Tsutsui, K., Yamada, T., Kimura, M., Nakano, I., Shimono, C., Sanzen, N., Furutani, Y., Fukuda, T., Oguri, Y., Shimamoto, K., Kiyozumi, D., Sato, Y., Sado, Y., Senoo, H., Yamashina, S., Fukuda, S., Kawai, J., Sugiura, N., Kimata, K., Hayashizaki, Y., and Sekiguchi, K. (2008) Transcriptome-based systematic identification of extracellular matrix proteins. *Proc. Natl. Acad. Sci. U.S.A.* **105,** 12849–12854
22. Kikkawa, Y., Sanzen, N., Fujiwara, H., Sonnenberg, A., and Sekiguchi, K. (2000) Integrin binding specificity of laminin-10/11. Laminin-10/11 are recognized by α3β1, α6β1, and α6β4 integrins. *J. Cell Sci.* **113,** 869–876
23. Manabe, R., Ohe, N., Maeda, T., Fukuda, T., and Sekiguchi, K. (1997) Modulation of cell-adhesive activity of fibronectin by the alternatively spliced EDA segment. *J. Cell Biol.* **139,** 295–307
24. Katayama, M., Sanzen, N., Funakoshi, A., and Sekiguchi, K. (2003) Laminin γ2-chain fragment in the circulation. A prognostic indicator of epithelial tumor invasion. *Cancer Res.* **63,** 222–229
25. Takagi, J., Erickson, H. P., and Springer, T. A. (2001) C-terminal opening mimics "inside-out" activation of integrin α5β1. *Nat. Struct. Biol.* **8,** 412–416
26. Sekiguchi, K., Hakomori, S., Funahashi, M., Matsumoto, I., and Seno, N. (1983) Binding of fibronectin and its proteolytic fragments to glycosaminoglycans. Exposure of cryptic glycosaminoglycan-binding domains upon limited proteolysis. *J. Biol. Chem.* **258,** 14359–14365
27. Kozaki, T., Matsui, Y., Gu, J., Nishiuchi, R., Sugiura, N., Kimata, K., Ozono, K., Yoshikawa, H., and Sekiguchi, K. (2003) Recombinant expression and characterization of a novel fibronectin isoform expressed in cartilaginous tissues. *J. Biol. Chem.* **278,** 50546–50553
28. Laemmli, U. K. (1970) Cleavage of structural proteins during the assembly of the head of bacteriophage T4. *Nature* **227,** 680–685
29. Edman, K. A. (1950) The action of ouabain on heart actomyosin. *Acta Physiol. Scand.* **21,** 230–237
30. Sato, Y., Uemura, T., Morimitsu, K., Sato-Nishiuchi, R., Manabe, R., Takagi, J., Yamada, M., and Sekiguchi, K. (2009) Molecular basis of the recognition of nephronectin by integrin α8β1. *J. Biol. Chem.* **284,** 14524–14536
31. Nishiuchi, R., Takagi, J., Hayashi, M., Ido, H., Yagi, Y., Sanzen, N., Tsuji, T., Yamada, M., and Sekiguchi, K. (2006) Ligand-binding specificities of laminin-binding integrins. A comprehensive survey of laminin-integrin interactions using recombinant α3β1, α6β1, α7β1, and α6β4 integrins. *Matrix Biol.* **25,** 189–197
32. Nishiuchi, R., Murayama, O., Fujiwara, H., Gu, J., Kawakami, T., Aimoto, S., Wada, Y., and Sekiguchi, K. (2003) Characterization of the ligand-binding specificities of integrin α3β1 and α6β1 using a panel of purified laminin isoforms containing distinct α chains. *J. Biochem.* **134,** 497–504
33. Ito, K., Kon, S., Nakayama, Y., Kurotaki, D., Saito, Y., Kanayama, M., Kimura, C., Diao, H., Morimoto, J., Matsui, Y., and Uede, T. (2009) The differential amino acid requirement within osteopontin in α4 and α9 integrin-mediated cell binding and migration. *Matrix Biol.* **28,** 11–19
34. Gupta, S. K., and Vlahakis, N. E. (2009) Integrin α9β1 mediates enhanced cell migration through nitric-oxide synthase activity regulated by Src tyrosine kinase. *J. Cell Sci.* **122,** 2043–2054
35. Yokosaki, Y., Matsuura, N., Higashiyama, S., Murakami, I., Obara, M., Yamakido, M., Shigeto, N., Chen, J., and Sheppard, D. (1998) Identification of the ligand binding site for the integrin α9β1 in the third fibronectin type III repeat of tenascin-C. *J. Biol. Chem.* **273,** 11423–11428
36. Yokosaki, Y., Matsuura, N., Sasaki, T., Murakami, I., Schneider, H., Higashiyama, S., Saitoh, Y., Yamakido, M., Taooka, Y., and Sheppard, D. (1999) The integrin $\alpha_9\beta_1$ binds to a novel recognition sequence (SVVYGLR) in the thrombin-cleaved amino-terminal fragment of osteopontin. *J. Biol. Chem.* **274,** 36328–36334
37. Eto, K., Puzon-McLaughlin, W., Sheppard, D., Sehara-Fujisawa, A., Zhang, X. P., and Takada, Y. (2000) RGD-independent binding of integrin α9β1 to the ADAM-12 and -15 disintegrin domains mediates cell-cell interaction. *J. Biol. Chem.* **275,** 34922–34930
38. Verdone, G., Doliana, R., Corazza, A., Colebrooke, S. A., Spessotto, P., Bot, S., Bucciotti, F., Capuano, A., Silvestri, A., Viglino, P., Campbell, I. D., Colombatti, A., and Esposito, G. (2008) The solution structure of EMILIN1 globular C1q domain reveals a disordered insertion necessary for interaction with the α4β1 integrin. *J. Biol. Chem.* **283,** 18947–18956
39. Oommen, S., Gupta, S. K., and Vlahakis, N. E. (2011) Vascular endothelial growth factor A (VEGF-A) induces endothelial and cancer cell migration through direct binding to integrin α9β1. Identification of a specific α9β1 binding site. *J. Biol. Chem.* **286,** 1083–1092
40. Danussi, C., Petrucco, A., Wassermann, B., Pivetta, E., Modica, T. M., Del Bel Belluz, L., Colombatti, A., and Spessotto, P. (2011) EMILIN1-α4/α9 integrin interaction inhibits dermal fibroblast and keratinocyte proliferation. *J. Cell Biol.* **195,** 131–145
41. Colombatti, A., Bressan, G. M., Castellani, I., and Volpin, D. (1985) Glycoprotein 115, a glycoprotein isolated from chick blood vessels, is widely distributed in connective tissue. *J. Cell Biol.* **100,** 18–26
42. Pytela, R., Pierschbacher, M. D., and Ruoslahti, E. (1985) Identification and isolation of a 140-kDa cell surface glycoprotein with properties expected of a fibronectin receptor. *Cell* **40,** 191–198
43. Knight, C. G., Morton, L. F., Peachey, A. R., Tuckwell, D. S., Farndale, R. W., and Barnes, M. J. (2000) The collagen-binding A-domains of integrins $\alpha_1\beta^1$ and $\alpha_2\beta_1$ recognize the same specific amino acid sequence, GFOGER, in native (triple-helical) collagens. *J. Biol. Chem.* **275,** 35–40
44. Ido, H., Nakamura, A., Kobayashi, R., Ito, S., Li, S., Futaki, S., and Sekiguchi, K. (2007) The requirement of the glutamic acid residue at the third position from the carboxyl termini of the laminin γ chains in integrin binding by laminins. *J. Biol. Chem.* **282,** 11144–11154
45. Takagi, J. (2007) Structural basis for ligand recognition by integrins. *Curr. Opin. Cell Biol.* **19,** 557–564
46. Springer, T. A., Zhu, J., and Xiao, T. (2008) Structural basis for distinctive recognition of fibrinogen γC peptide by the platelet integrin αIIbβ3. *J. Cell Biol.* **182,** 791–800
47. Clements, J. M., Newham, P., Shepherd, M., Gilbert, R., Dudgeon, T. J., Needham, L. A., Edwards, R. M., Berry, L., Brass, A., and Humphries, M. J. (1994) Identification of a key integrin-binding sequence in VCAM-1 homologous to the LDV active site in fibronectin. *J. Cell Sci.* **107,** 2127–2135
48. Mould, A. P., and Humphries, M. J. (1991) Identification of a novel recognition sequence for the integrin α4β1 in the COOH-terminal heparin-binding domain of fibronectin. *EMBO J.* **10,** 4089–4095
49. Xiong, J. P., Stehle, T., Zhang, R., Joachimiak, A., Frech, M., Goodman, S. L., and Arnaout, M. A. (2002) Crystal structure of the extracellular segment of integrin αVβ3 in complex with an Arg-Gly-Asp ligand. *Science* **296,** 151–155
50. Schwarz, R. S., Bosch, T. C., and Cadavid, L. F. (2008) Evolution of polydom-like molecules. Identification and characterization of cnidarian polydom (Cnpolydom) in the basal metazoan Hydractinia. *Dev. Comp. Immunol.* **32,** 1192–1210
51. Brown, N. H. (2000) Cell-cell adhesion via the ECM. Integrin genetics in fly and worm. *Matrix Biol.* **19,** 191–201
52. Hynes, R. O. (1992) Integrins. Versatility, modulation, and signaling in cell adhesion. *Cell* **69,** 11–25
53. Hynes, R. O. (2002) Integrins. Bidirectional, allosteric signaling machines. *Cell* **110,** 673–687
54. Meredith, J. E., Jr., Winitz, S., Lewis, J. M., Hess, S., Ren, X. D., Renshaw, M. W., and Schwartz, M. A. (1996) The regulation of growth and intracellular signaling by integrins. *Endocr. Rev.* **17,** 207–220
55. Gu, J., Sumida, Y., Sanzen, N., and Sekiguchi, K. (2001) Laminin-10/11 and fibronectin differentially regulate integrin-dependent Rho and Rac activation via $p130^{Cas}$-CrkII-DOCK180 pathway. *J. Biol. Chem.* **276,** 27090–27097
56. Danen, E. H., Sonneveld, P., Brakebusch, C., Fassler, R., and Sonnenberg, A. (2002) The fibronectin-binding integrins α5β1 and αvβ3 differentially modulate RhoA-GTP loading, organization of cell matrix adhesions, and fibronectin fibrillogenesis. *J. Cell Biol.* **159,** 1071–1086

57. deHart, G. W., Jin, T., McCloskey, D. E., Pegg, A. E., and Sheppard, D. (2008) The α9β1 integrin enhances cell migration by polyamine-mediated modulation of an inward-rectifier potassium channel. *Proc. Natl. Acad. Sci. U.S.A.* **105,** 7188–7193
58. Saini, A., Seller, Z., Davies, D., Marshall, J. F., and Hart, I. R. (1997) Activation status and function of the VLA-4 (α4β1) integrin expressed on human melanoma cell lines. *Int. J. Cancer* **73,** 264–270
59. Komoriya, A., Green, L. J., Mervic, M., Yamada, S. S., Yamada, K. M., and Humphries, M. J. (1991) The minimal essential sequence for a major cell type-specific adhesion site (CS1) within the alternatively spliced type III connecting segment domain of fibronectin is leucine-aspartic acid-valine. *J. Biol. Chem.* **266,** 15075–15079

Polydom/SVEP1 Is a Ligand for Integrin α9β1

Ryoko Sato-Nishiuchi, Itsuko Nakano, Akio Ozawa, Yuya Sato, Makiko Takeichi, Daiji Kiyozumi, Kiyoshi Yamazaki, Teruo Yasunaga, Sugiko Futaki and Kiyotoshi Sekiguchi

J. Biol. Chem. 2012, 287:25615-25630.
doi: 10.1074/jbc.M112.355016 originally published online May 31, 2012

SUPPLEMENTARY INFORMATION

Polydom/SVEP1 is a ligand for integrin α9β1

Ryoko Sato-Nishiuchi *et al.*

SUPPLEMENTARY FIGURE LEGENDS

FIGURE S1. **Immunohistochemical detection of polydom with an anti-pol-C antibody.** *A* to *C*, cryosections of mouse E16.5 embryos were stained with an anti-pol-C antibody. Representative images of the stomach (*A*), intestine (*B*), and lung (*C*) are shown. The *insets* are magnified views of the *boxed areas*. *D* to *F*, no signals are detected with normal rabbit IgG. *Bars*, 100 μm.

FIGURE S2. **Flow cytometric analysis of integrin α9β1 expression.** *A*, A549, HT1080, and RD cells were labeled with an anti-integrin α9β1 mAb (Y9A2) or control mouse IgG, and then subjected to flow cytometric analysis. Integrin α9β1 is expressed on RD cells, but not on A549 or HT1080 cells. *B*, RD cells treated with either a control siRNA (*Control*) or an integrin α9 siRNA (*α9 KD*) were labeled with an anti-integrin α9β1 mAb (Y9A2) or control mouse IgG and subjected to flow cytometric analysis. Untreated RD cells (*None*) were also analyzed. The expression level of integrin α9β1 is significantly reduced in the integrin α9 siRNA-treated cells.

FIGURE S3. **Multiple sequence alignments by ClustalW of the 34 CCP domains of mouse polydom.** Only CCP21 has an extra ~40-amino acid insertion.

FIGURE S4. **Double immunofluorescence detection of tenascin-C and integrin α9β1 ligands in tissues.** *A* to *F*, cryosections of mouse E16.5 embryos were incubated with recombinant integrin α9β1 in the presence of 1 mM $MnCl_2$ (*A*, *D*) together with an anti-tenascin-C antibody (*B*, *E*). Representative images of the stomach (*A–C*) and lung (*D–F*) are shown. The integrin signals are partially colocalized with those of tenascin-C (*arrowheads*). Note that the mesenchyme positive for integrin α9β1 ligands is often negative for tenascin-C (*asterisks*). The smooth muscle layer surrounding the trachea is strongly positive for bound integrin α9β1, but negative for tenascin-C (*F*, *arrow*). *Bar*, 100 μm.

FIGURE S5. **Multiple sequence alignments of the β-propeller domain of the integrin αV, α4 and α9 subunits.** *A*, multiple sequence alignments by ClustalW of the human integrin αV, α4, and α9 subunits. The sequences between blades 2 to 4 of the β-propeller domain are shown. The two Asp residues indicated by *arrowheads* have been shown to form salt bridges with the Arg residue of an RGD-containing ligand (49). These acidic residues are apparently replaced by Lys and Arg residues (highlighted in *gray*) in the integrin α4 and α9 subunits. *B* and *C*, multiple sequence alignments by ClustalW of the integrin α4 (*B*), and α9 (*C*) subunits of different species (the full-length sequence of zebrafish α9 has not been reported, and therefore the sequence of medaka α9 is presented). The basic residues indicated in (*A*) are conserved within vertebrates.

FIGURE S6. **Multiple sequence alignments of CCP21 domains.** Multiple sequence alignments by ClustalW of the CCP21 domains of mouse, human, chimpanzee, horse, dog, bovine, pig, rabbit, rat, chicken, xenopus and zebrafish polydom are shown. The EDDMMEVPY sequence in the extra ~40-amino acid segment (*underlined*) of CCP21 is well conserved in mammals. However, the EDDMMEVPY sequence is absent from in non-mammals.

Figure S1

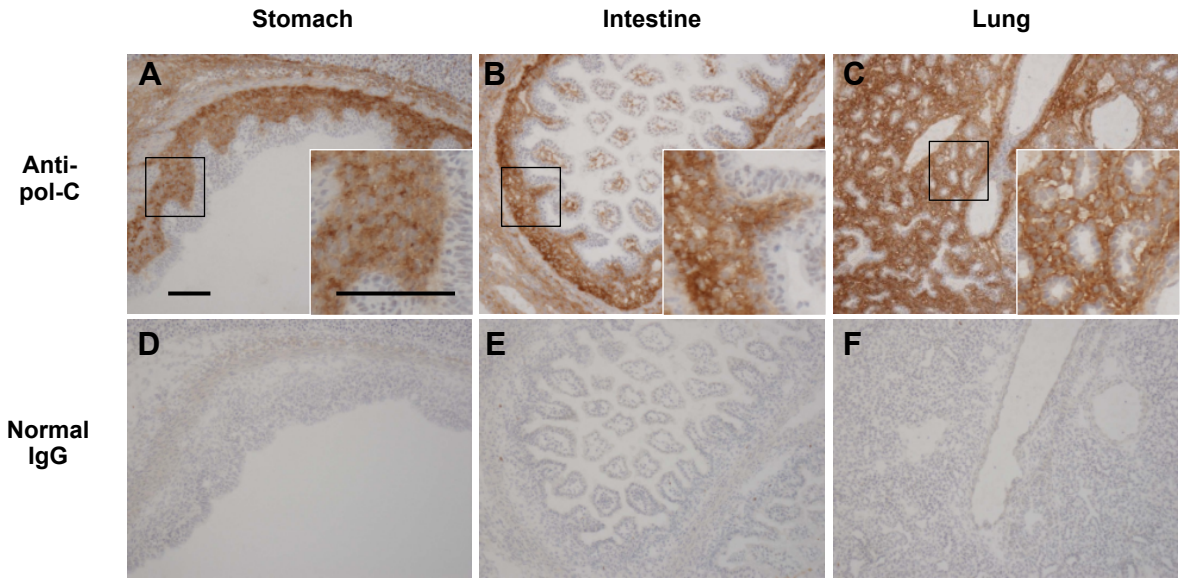

Figure S2

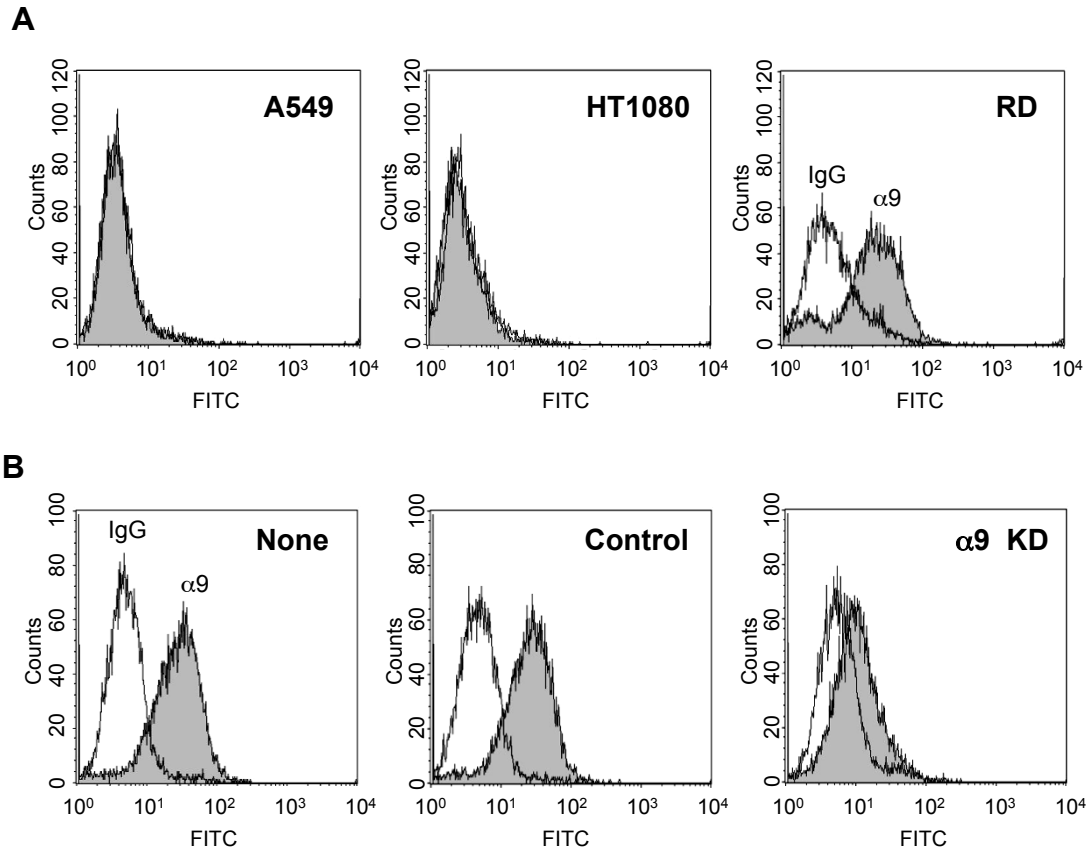
A
A549
HT1080
RD
IgG
α9
Counts
FITC
B
None
Control
α9 KD
IgG
α9
Counts
FITC

Figure S3

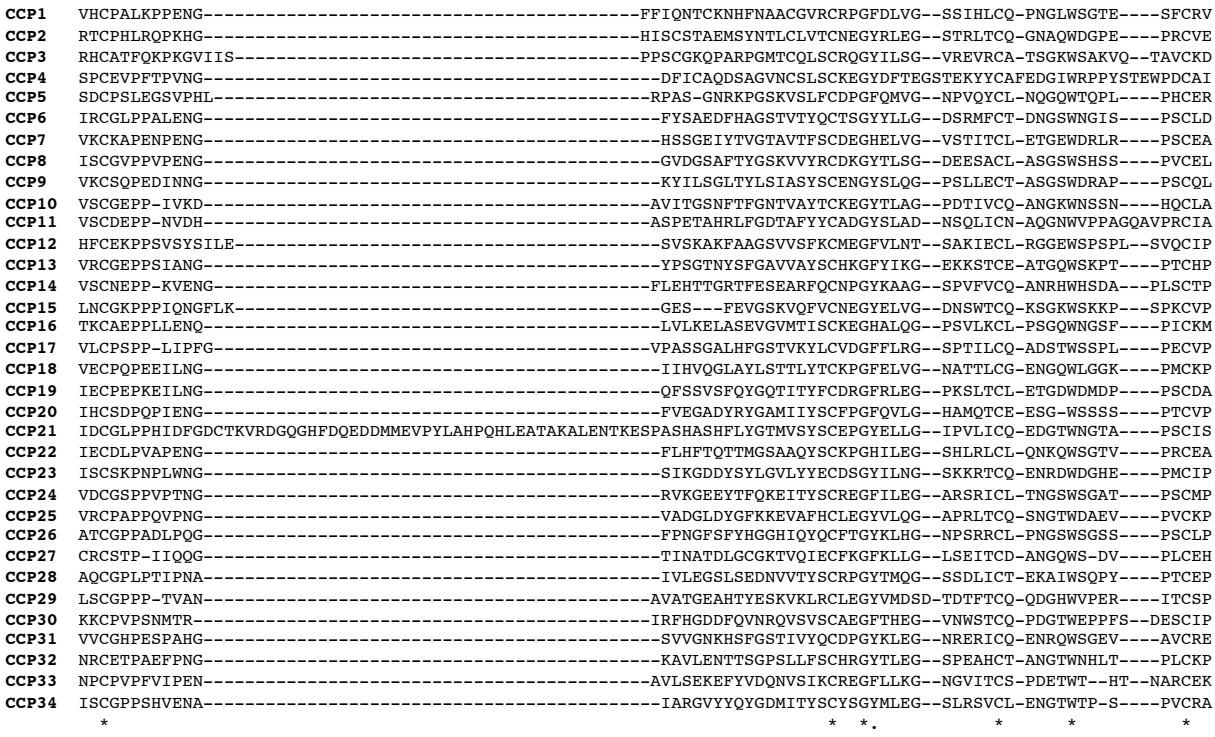
CCP1 VHCPALKPPENG----------FFIQNTCKNHFNAACGVRCRPGFDLVG--SSIHLCQ-PNGLWSGTE----SFCRV
CCP2 RTCPHLRQPKHG----------HISCSTAEMSYNTLCLVTCNEGYRLEG--STRLTCQ-GNAQWDGPE----PRCVE
CCP3 RHCATFQKPKGVIIS----------PPSCGKQPARPGMTCQLSCRQGYILSG--VREVRCA-TSGKWSAKVQ--TAVCKD
CCP4 SPCEVPFTPVNG----------DFICAQDSAGVNCSLSCKEGYDFTEGSTEKYYCAFEDGIWRPPYSTEWPDCAI
CCP5 SDCPSLEGSVPHL----------RPAS-GNRKPGSKVSLFCDPGFQMVG--NPVQYCL-NQGQWTQPL----PHCER
CCP6 IRCGLPPALENG----------FYSAEDFHAGSTVTYQCTSGYYLLG--DSRMFCT-DNGSWNGIS----PSCLD
CCP7 VKCKAPENPENG----------HSSGEIYTVGTAVTFSCDEGHELVG--VSTITCL-ETGEWDRLR----PSCEA
CCP8 ISCGVPPVPENG----------GVDGSAFTYGSKVVYRCDKGYTLSG--DEESACL-ASGSWSHSS----PVCEL
CCP9 VKCSQPEDINNG----------KYILSGLTYLSIASYSCENGYSLQG--PSLLECT-ASGSWDRAP----PSCQL
CCP10 VSCGEPP-IVKD----------AVITGSNFTFGNTVAYTCKEGYTLAG--PDTIVCQ-ANGKWNSSN----HQCLA
CCP11 VSCDEPP-NVDH----------ASPETAHRLFGDTAFYYCADGYSLAD--NSQLICN-AQGNWVPPAGQAVPRCIA
CCP12 HFCEKPPSVSYSILE----------SVSKAKFAAGSVVSFKCMEGFVLNT--SAKIECL-RGGEWSPSPL--SVQCIP
CCP13 VRCGEPPSIANG----------YPSGTNYSFGAVVAYSCHKGFYIKG--EKKSTCE-ATGQWSKPT----PTCHP
CCP14 VSCNEPP-KVENG----------FLEHTTGRTFESEARFQCNPGYKAAG--SPVFVCQ-ANRHWHSDA---PLSCTP
CCP15 LNCGKPPPIQNGFLK----------GES---FEVGSKVQFVCNEGYELVG--DNSWTCQ-KSGKWSKKP---SPKCVP
CCP16 TKCAEPPLLENQ----------LVLKELASEVGVMTISCKEGHALQG--PSVLKCL-PSGQWNGSF----PICKM
CCP17 VLCPSPP-LIPFG----------VPASSGALHFGSTVKYLCVDGFFLRG--SPTILCQ-ADSTWSSPL----PECVP
CCP18 VECPQPEEILNG----------IIHVQGLAYLSTTLYTCKPGFELVG--NATTLCG-ENGQWLGGK----PMCKP
CCP19 IECPEPKEILNG----------QFSSVSFQYGQTITYFCDRGFRLEG--PKSLTCL-ETGDWDMDP----PSCDA
CCP20 IHCSDPQPIENG----------FVEGADYRYGAMIIYSCFPGFQVLG--HAMQTCE-ESG-WSSSS----PTCVP
CCP21 IDCGLPPHIDFGDCTKVRDGQGHFDQEDDMMEVPYLAHPQHLEATAKALENTKESPASHASHFLYGTMVSYSCEPGYELLG--IPVLICQ-EDGTWNGTA----PSCIS
CCP22 IECDLPVAPENG----------FLHFTQTTMGSAAQYSCKPGHILEG--SHLRLCL-QNKQWSGTV----PRCEA
CCP23 ISCSKPNPLWNG----------SIKGDDYSYLGVLYYECDSGYILNG--SKKRTCQ-ENRDWDGHE----PMCIP
CCP24 VDCGSPPVPTNG----------RVKGEEYTFQKEITYSCREGFILEG--ARSRICL-TNGSWSGAT----PSCMP
CCP25 VRCPAPPQVPNG----------VADGLDYGFKKEVAFHCLEGYVLQG--APRLTCQ-SNGTWDAEV----PVCKP
CCP26 ATCGPPADLPQG----------FPNGFSFYHGGHIQYQCFTGYKLHG--NPSRRCL-PNGSWSGSS----PSCLP
CCP27 CRCSTP-IIQQG----------TINATDLGCGKTVQIECFKGFKLLG--LSEITCD-ANGQWS-DV----PLCEH
CCP28 AQCGPLPTIPNA----------IVLEGSLSEDNVVTYSCRPGYTMQG--SSDLICT-EKAIWSQPY----PTCEP
CCP29 LSCGPPP-TVAN----------AVATGEAHTYESKVKLRCLEGYVMDSD-TDTFTCQ-QDGHWVPER----ITCSP
CCP30 KKCPVPSNMTR----------IRFHGDDFQVNRQVSVSCAEGFTHEG--VNWSTCQ-PDGTWEPPFS--DESCIP
CCP31 VVCGHPESPAHG----------SVVGNKHSFGSTIVYQCDPGYKLEG--NRERICQ-ENRQWSGEV----AVCRE
CCP32 NRCETPAEFPNG----------KAVLENTTSGPSLLFSCHRGYTLEG--SPEAHCT-ANGTWNHLT----PLCKP
CCP33 NPCPVPFVIPEN----------AVLSEKEFYVDQNVSIKCREGFLLKG--NGVITCS-PDETWT--HT--NARCEK
CCP34 ISCGPPSHVENA----------IARGVYYQYGDMITYSCYSGYMLEG--SLRSVCL-ENGTWTP-S----PVCRA

Figure S4

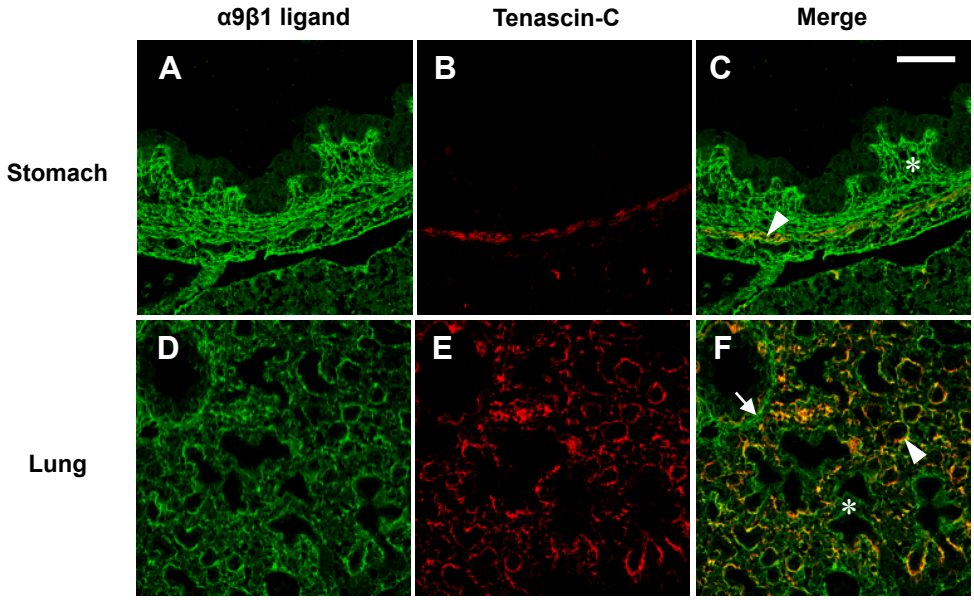

Figure S5

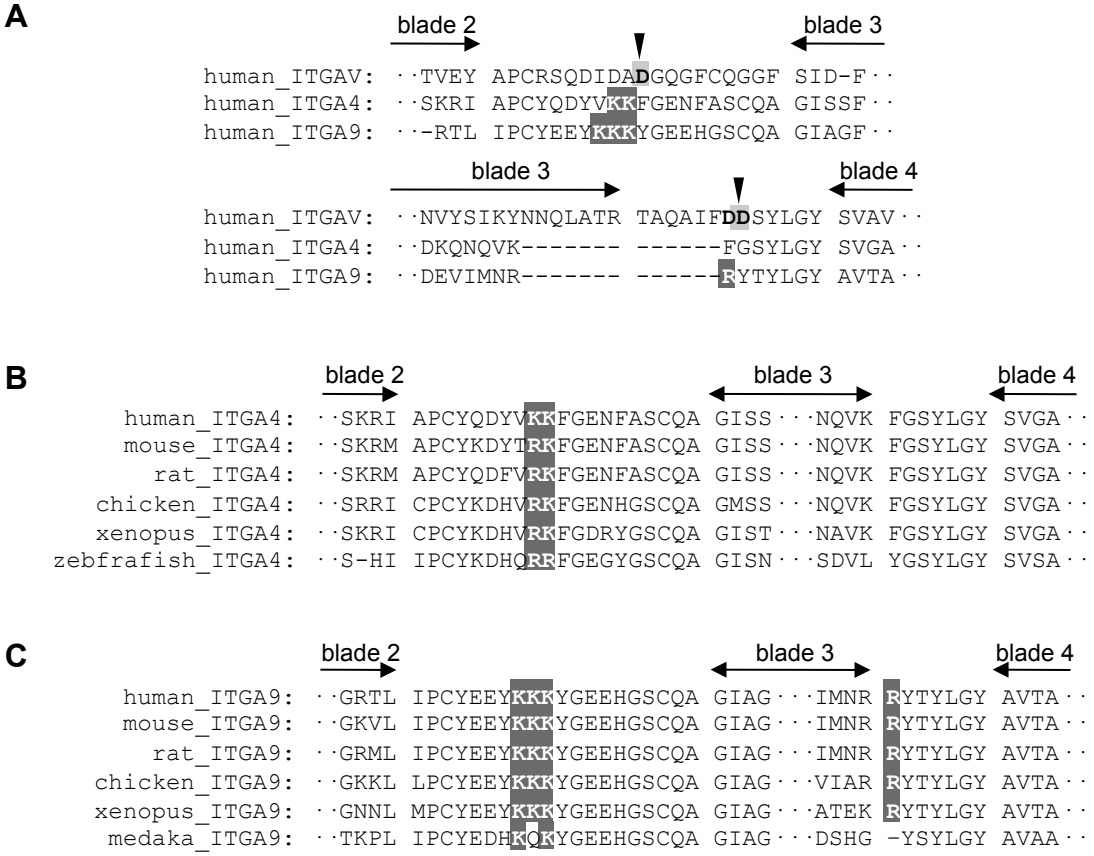
A
blade 2
blade 3
human_ITGAV: ··TVEY APCRSQDIDADGQGFCQGGF SID-F··
human_ITGA4: ··SKRI APCYQDYVKKFGENFASCQA GISSF··
human_ITGA9: ··-RTL IPCYEEYKKKYGEEHGSCQA GIAGF··
blade 3
blade 4
human_ITGAV: ··NVYSIKYNNQLATR TAQAIFDDSYLGY SVAV··
human_ITGA4: ··DKQNQVK------- ------FGSYLGY SVGA··
human_ITGA9: ··DEVIMNR------- ------RYTYLGY AVTA··
B
blade 2
blade 3
blade 4
human_ITGA4: ··SKRI APCYQDYVKKFGENFASCQA GISS···NQVK FGSYLGY SVGA··
mouse_ITGA4: ··SKRM APCYKDYTRKFGENFASCQA GISS···NQVK FGSYLGY SVGA··
rat_ITGA4: ··SKRM APCYQDFVRKFGENFASCQA GISS···NQVK FGSYLGY SVGA··
chicken_ITGA4: ··SRRI CPCYKDHVRKFGENHGSCQA GMSS···NQVK FGSYLGY SVGA··
xenopus_ITGA4: ··SKRI CPCYKDHVRKFGDRYGSCQA GIST···NAVK FGSYLGY SVGA··
zebfrafish_ITGA4: ··S-HI IPCYKDHQRRFGEGYGSCQA GISN···SDVL YGSYLGY SVSA··
C
blade 2
blade 3
blade 4
human_ITGA9: ··GRTL IPCYEEYKKKYGEEHGSCQA GIAG···IMNR RYTYLGY AVTA··
mouse_ITGA9: ··GKVL IPCYEEYKKKYGEEHGSCQA GIAG···IMNR RYTYLGY AVTA··
rat_ITGA9: ··GRML IPCYEEYKKKYGEEHGSCQA GIAG···IMNR RYTYLGY AVTA··
chicken_ITGA9: ··GKKL LPCYEEYKKKYGEEHGSCQA GIAG···VIAR RYTYLGY AVTA··
xenopus_ITGA9: ··GNNL MPCYEEYKKKYGEEHGSCQA GIAG···ATEK RYTYLGY AVTA··
medaka_ITGA9: ··TKPL IPCYEDHKQKYGEEHGSCQA GIAG···DSHG -YSYLGY AVAA··

Figure S6

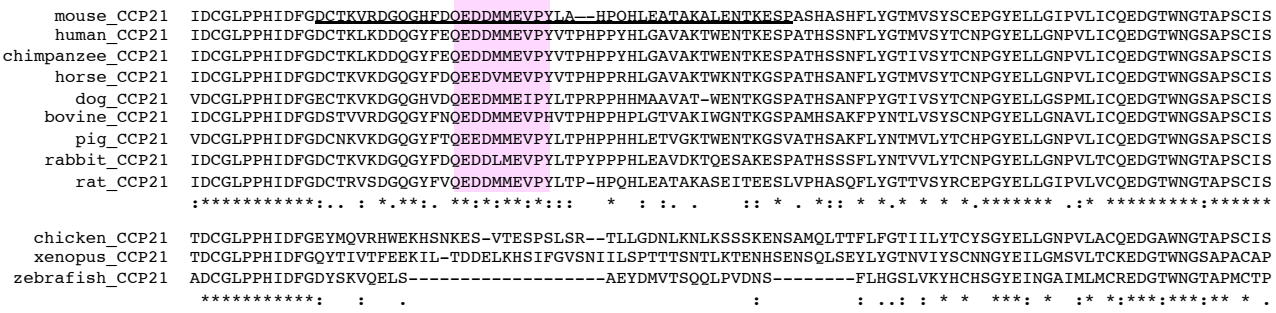
mouse_CCP21 IDCGLPPHIDFGDCTKVRDGOGHFDQEDDMMEVPYLA--HPQHLEATAKALENTKESPASHASHFLYGTMVSYSCEPGYELLGIPVLICQEDGTWNGTAPSCIS
human_CCP21 IDCGLPPHIDFGDCTKLKDDQGYFEQEDDMMEVPYVTPHPPYHLGAVAKTWENTKESPATHSSNFLYGTMVSYTCNPGYELLGNPVLICQEDGTWNGSAPSCIS
chimpanzee_CCP21 IDCGLPPHIDFGDCTKLKDDQGYFEQEDDMMEVPYVTPHPPYHLGAVAKTWENTKESPATHSSNFLYGTIVSYTCNPGYELLGNPVLICQEDGTWNGSAPSCIS
horse_CCP21 IDCGLPPHIDFGDCTKVKDGQGYFDQEEDVMEVPYVTPHPPRHLGAVAKTWKNTKGSPATHSANFLYGTMVSYTCNPGYELLGNPVLICQEDGTWNGSAPSCIS
dog_CCP21 VDCGLPPHIDFGECTKVKDGQGHVDQEEDMMEIPYLTPRPPHHMAAVAT-WENTKGSPATHSANFPYGTIVSYTCNPGYELLGSPMLICQEDGTWNGSAPSCIS
bovine_CCP21 IDCGLPPHIDFGDSTVVRDGQGYFNQEDDMMEVPHVTPHPPHPLGTVAKIWGNTKGSPAMHSAKFPYNTLVSYSCNPGYELLGNAVLICQEDGTWNGSAPSCIS
pig_CCP21 VDCGLPPHIDFGDCNKVKDGQGYFTQEEDMMEVPYLTPHPPHHLETVGKTWENTKGSVATHSAKFLYNTMVLYTCHPGYELLGNPVLICQEDGTWNGSAPSCIS
rabbit_CCP21 IDCGLPPHIDFGDCTKVKDGQGYFDQEDDLMEVPYLTPYPPPHLEAVDKTQESAKESPATHSSSFLYNTVVLYTCNPGYELLGNPVLTCQEDGTWNGTAPSCIS
rat_CCP21 IDCGLPPHIDFGDCTRVSDGQGYFVQEDDMMEVPYLTP-HPQHLEATAKASEITEESLVPHASQFLYGTTVSYRCEPGYELLGIPVLVCQEDGTWNGTAPSCIS
:***********:.. : *.**:. **:*:**:*::: * : :. . :: * . *:: * *.* * * *.******* .:* *********:******
chicken_CCP21 TDCGLPPHIDFGEYMQVRHWEKHSNKES-VTESPSLSR--TLLGDNLKNLKSSSKENSAMQLTTFLFGTIILYTCYSGYELLGNPVLACQEDGAWNGTAPSCIS
xenopus_CCP21 TDCGLPPHIDFGQYTIVTFEEKIL-TDDELKHSIFGVSNIILSPTTTSNTLKTENHSENSQLSEYLYGTNVIYSCNNGYEILGMSVLTCKEDGTWNGSAPACAP
zebrafish_CCP21 ADCGLPPHIDFGDYSKVQELS-------------------AEYDMVTSQQLPVDNS--------FLHGSLVKYHCHSGYEINGAIMLMCREDGTWNGTAPMCTP
********** : . : : ..: : * * ***: * :* *:***:***:** * .